325
9/10/64

PWAC-429

EXPERIMENTAL RESULTS OF FORCED CONVECTION BOILING POTASSIUM HEAT TRANSFER AND PRESSURE DROP TESTS

AEC RESEARCH AND DEVELOPMENT REPORT

PRATT & WHITNEY AIRCRAFT
DIVISION OF UNITED AIRCRAFT CORPORATION
CANEL
MIDDLETOWN CONNECTICUT

TID-4500 (31st Ed.) CATEGORY UC-80
REACTOR TECHNOLOGY

PWAC-429
EXPERIMENTAL RESULTS OF FORCED CONVECTION BOILING POTASSIUM HEAT TRANSFER AND PRESSURE DROP TESTS

AEC RESEARCH AND DEVELOPMENT REPORT

CONTRACT
AT(30-1)-2789

Issued
July 16, 1964

Printed in U.S.A. Price ~~$2.00.~~ Available from the Office of
Technical Services, Department of Commerce,
Washington 25, D.C.

PRATT & WHITNEY AIRCRAFT
DIVISION OF UNITED AIRCRAFT CORPORATION
CANEL
MIDDLETOWN CONNECTICUT

TABLE OF CONTENTS

Page No.

TABLE OF FIGURES

EXPERIMENTAL RESULTS OF FORCED CONVECTION BOILING POTASSIUM HEAT TRANSFER AND PRESSURE DROP TESTS

Prepared By: E. Bernstein
J. P. Petrek
G. J. Rose
J. J. Horan

Approved By: D G Randall
D. G. Randall

H Means
H. E. Means

R. W. Kelly
R. W. Kelly

UNCLASSIFIED	H Means	July 9, 1964
CLASSIFICATION	AUTHORIZED CLASSIFIER	DATE

I. ABSTRACT

Experimental forced-convection boiling potassium heat transfer and pressure drop data were obtained at 1725F in a horizontal zero gravity boiler tube. System stability tests were conducted and the results compared with an electric analog of the system. A distinct condensing interface was observed in the condenser. This is illustrated in Fig. 1.

CONDENSER SECTION

NOTE: DISTINCT CONDENSING INTERFACE CAN BE OBSERVED

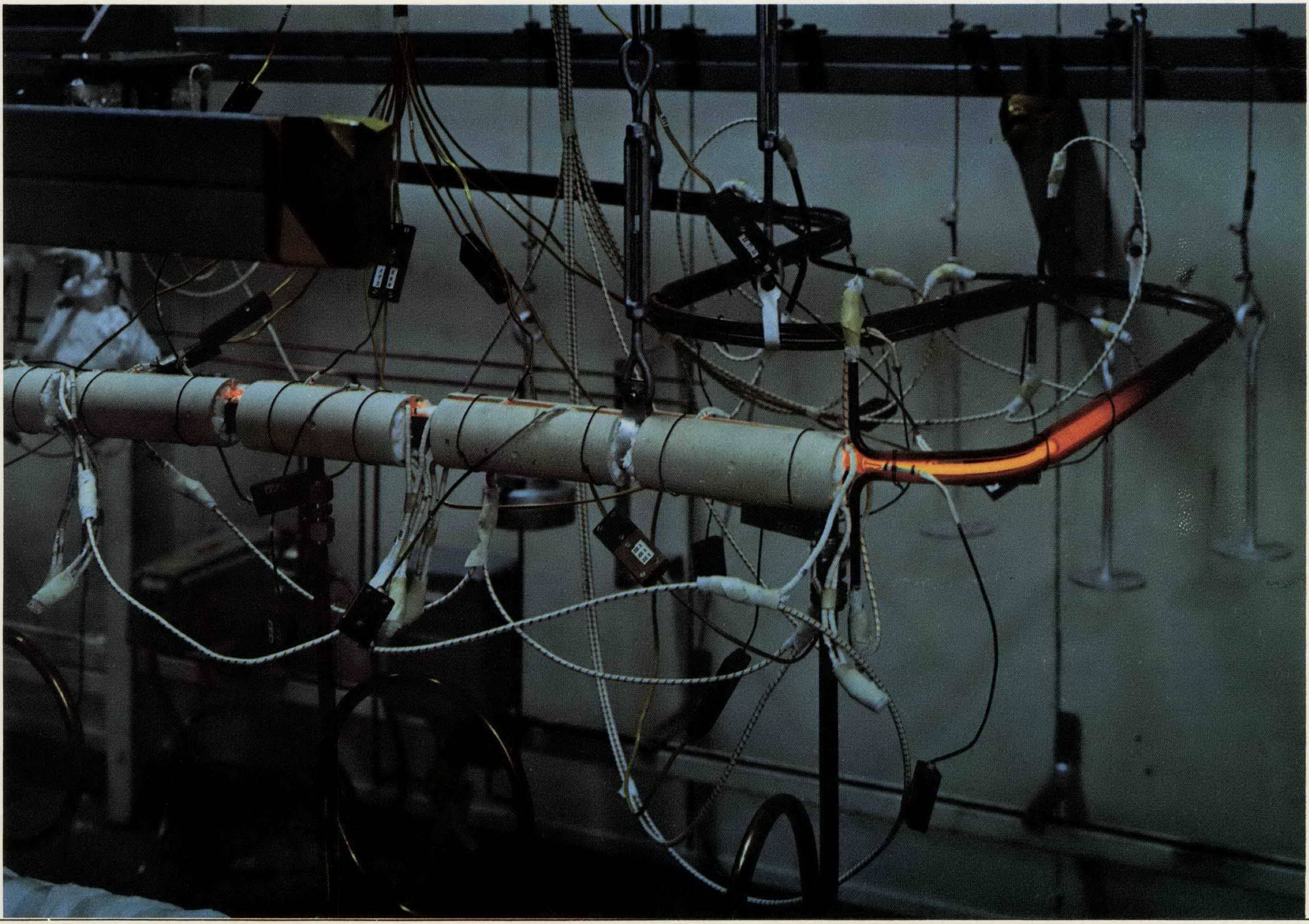

FIG 1

II. INTRODUCTION AND SUMMARY

Pratt & Whitney Aircraft-CANEL recently finished a series of forced-convection high temperature (1725F) boiling potassium heat transfer tests in a zero gravity serpentine boiler tube. The test-obtained data provides the boiler designer with a significant start in the design of a once-through alkali metal boiler for space applications. A promising full range boiling correlation is described in the Appendix.

The resistance to heat transfer in wet and dry vapor was defined to 100 percent vapor quality in a 0.186 inch diameter boiler tube, made of Haynes-25 alloy. Superheated vapor (to 74F) was obtained. Two-phase pressure drop data was simultaneously obtained and compared with theoretical correlations. The range of experimental parameters investigated are tabulated in Fig. 2.

The heat transfer data shown in Fig. 3 demonstrates the tremendous change in heat transfer rates between low and high quality potassium vapor. The dry vapor region virtually sizes the boiler. The pressure drop data, plotted in Fig. 4, shows the influence of vapor quality on pressure drop. The experimental pressure drop is compared with the Martinelli-Lockhart two-phase pressure drop correlation. The correlation is bounded (± 20 percent) by the experimental data. The boiler pressure drop has a strong influence on the size of the boiler, since the integrated driving force (ΔT) is significantly influenced by the pressure drop in the tube.

The localized nature of this data, as opposed to over-all data, allows the designer to use it over a wide range of pressures, temperatures, flow rates, heating fluids, heating methods and power conditions. The boiler designer utilizes this localized data by analytically traversing the length of the boiler tube, adjusting the resistance to heat transfer and fluid flow as the quality increases and recalculating the driving force (ΔT) for incremental lengths. These incremental lengths are integrated to obtain the required boiler tube length. Also, the system designer is now better able to select optimum temperature and flow levels. A typical result of this data is exemplified by the boiler mockup in Fig. 5.

In this experiment, a two-phase mixture was generated in a preboiler and vaporized an additional incremental amount in the test boiler. Heat was transferred to the test section by condensing potassium vapor on the shell side of the tube. Differential pressure measurement between the condensing potassium on the outside of the tube and the boiling potassium on the inside of the tube was converted to temperature differential by the application of the slope of the vapor pressure curve for potassium. The condensing resistance is near zero. The wall resistance was calculated using the Fourier heat conduction equation. Elimination of these resistances from the measured over-all resistance provided an accurate determination of the tube-side boiling heat transfer coefficient. A schematic description of the experimental technique is shown in Fig. 6. Photographs of the test boiler and experimental facility are shown in Figs. 7, 8, 9, and 10.

This experimental technique, employed by W. K. Woods at Massachusetts Institute of Technology in 1940, proved quite successful. It can be used to obtain local data for shell-side boiling, as in nuclear reactors, or tube side boiling, as employed in tube and shell heat exchangers. Some outstanding advantages of this experimental technique are:

1. Constant wall temperature data which is immediately applicable in the designer's equations.
2. The heat flux is precisely known and controlled, from which a heat transfer coefficient is calculated.
3. Simplicity and reliability of both the heaters and the instrumentation is of a high order.
4. Data is reproducible and highly accurate.
5. There is flexibility in selection of tube geometry or material.

FIG 2

RANGE OF EXPERIMENTAL PARAMETERS

Potassium Flow Rate, lb/hr	17-25
Vapor Quality, %	0-100
Boiling ΔT, F	2-170
Boiling Temperature, F	1625-1725
Heat Flux in Test Boiler, Btu/hr ft^2	17,000-52,000
Max. Heat Flux in Pre-Boiler	64,000
Boiling Pressure, psia	42-62
Max. Vapor Velocity, ft/sec	330
Test Duration, hr	3625
Boiling Hours	980

FIG 3

FORCED CONVECTION LOCAL BOILING HEAT TRANSFER COEFFICIENTS FOR POTASSIUM INSIDE A SERPENTINE TUBE

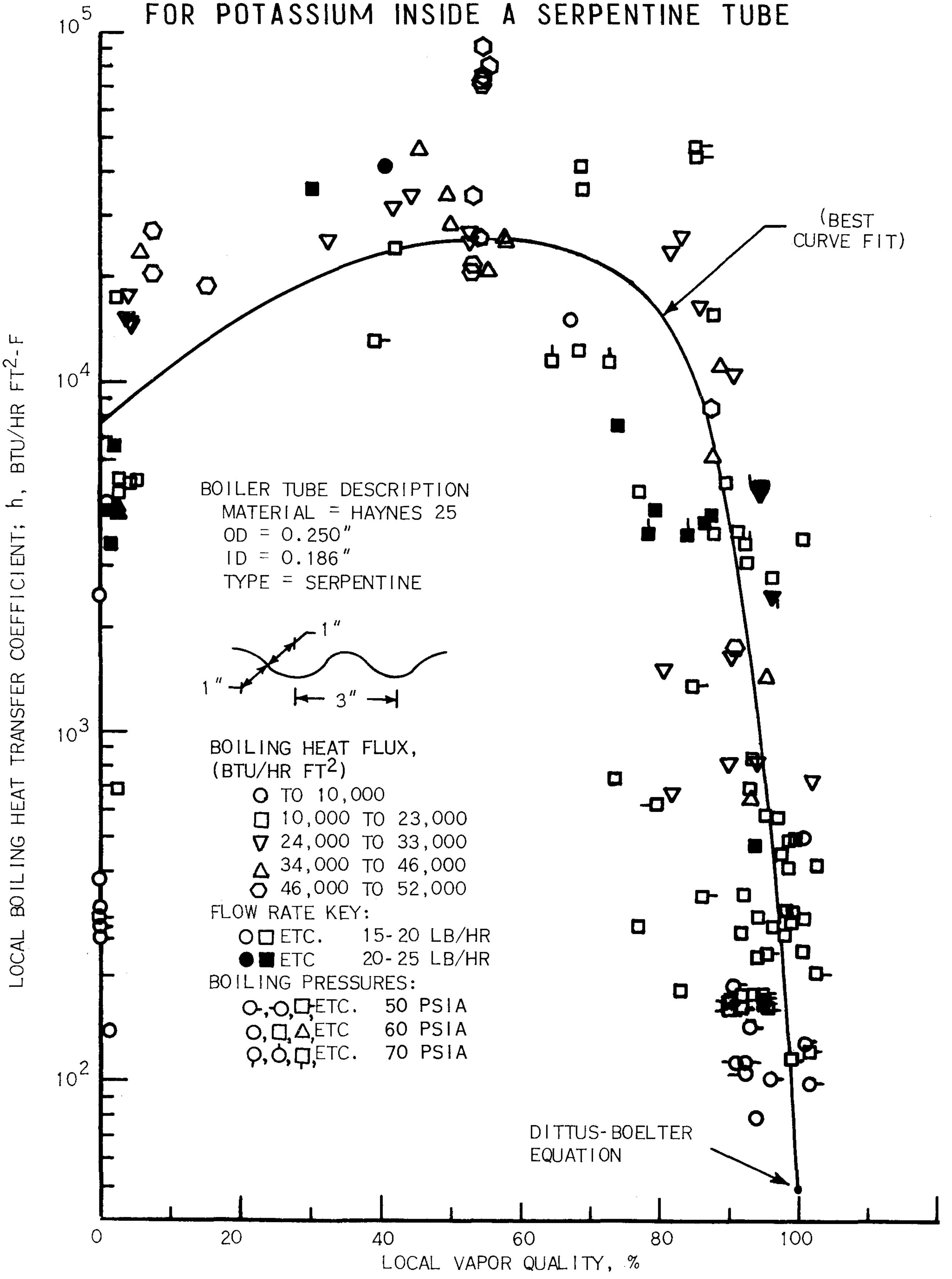

COMPARISON OF EXPERIMENTAL FORCED CONVECTION LOCAL BOILING PRESSURE COEFFICIENT WITH MARTINELLI-LOCKHART PRESSURE DROP CORRELATION

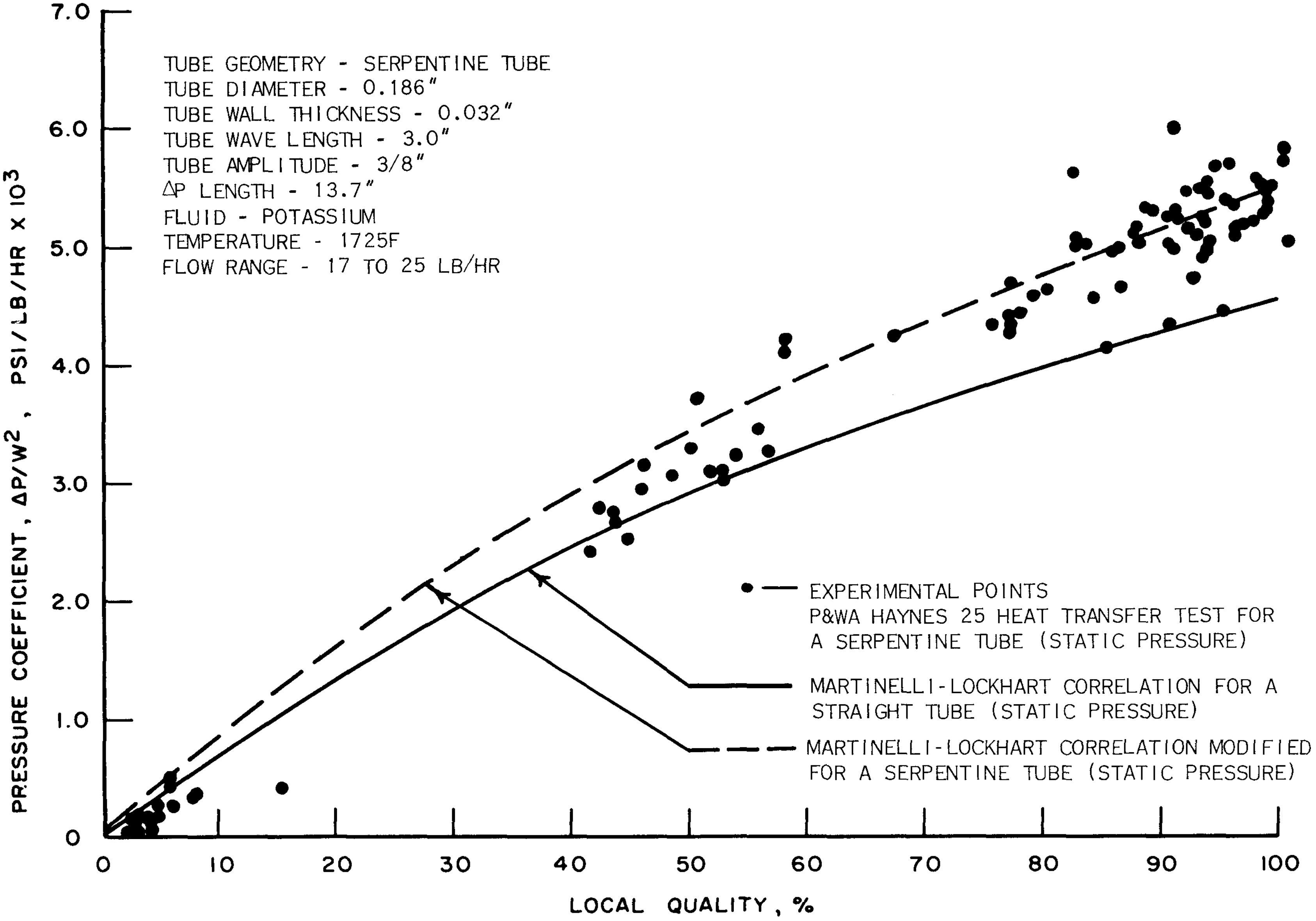

FIG 4

FIG 5

A-12762

SERPENTINE TUBE BOILER MOCK-UP

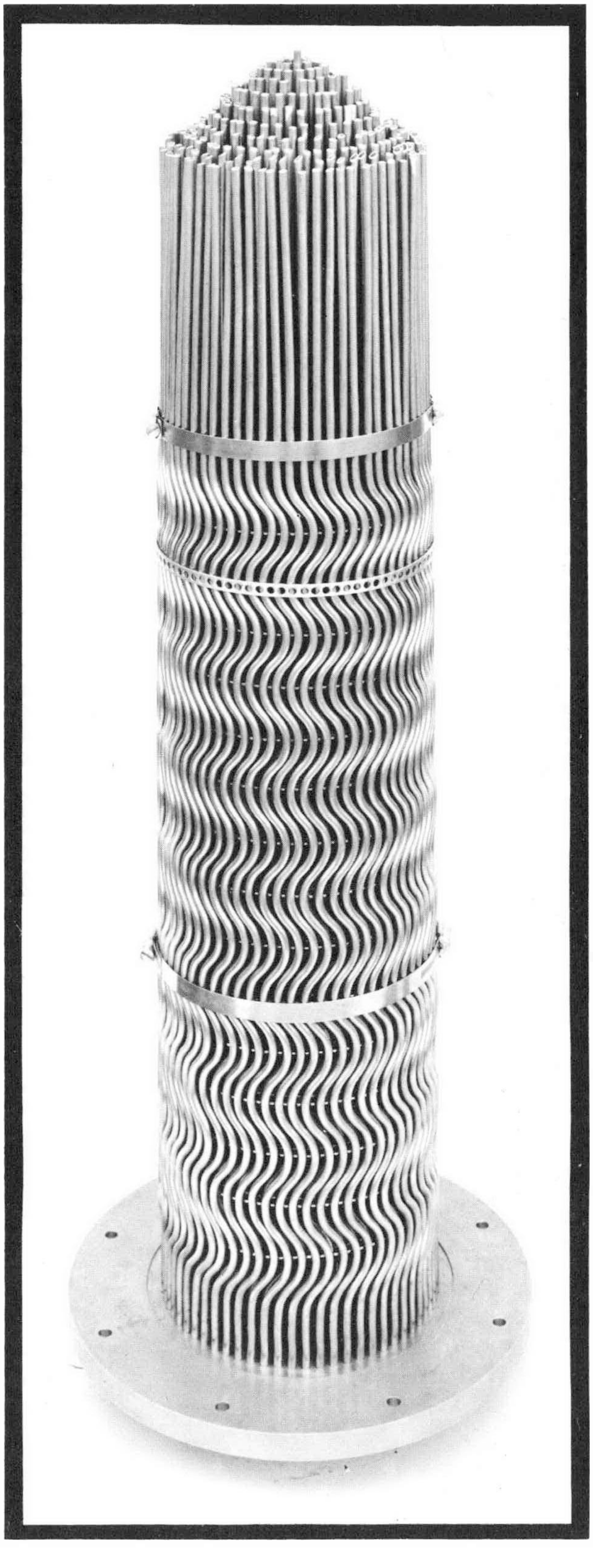

DESCRIPTION OF EXPERIMENTAL TECHNIQUE

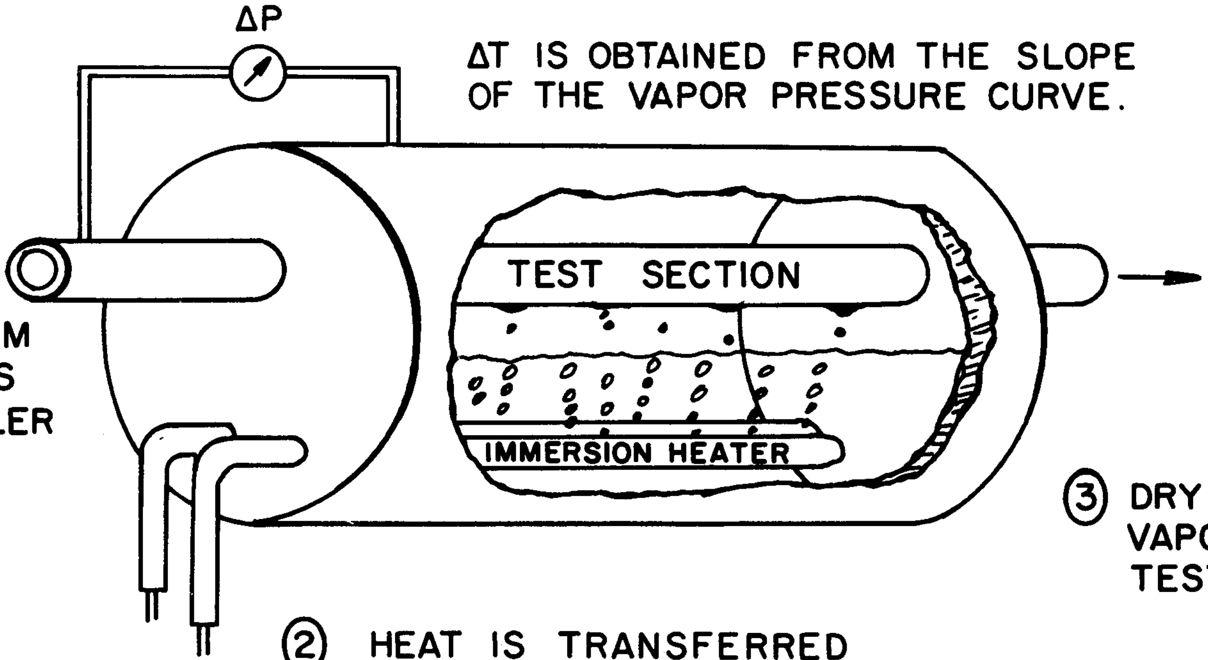

ΔT IS OBTAINED FROM THE SLOPE OF THE VAPOR PRESSURE CURVE.

① WET POTASSIUM VAPOR ENTERS FROM PREBOILER

② HEAT IS TRANSFERRED TO THE TEST SECTION BY CONDENSING POTASSIUM VAPOR ON THE OUTSIDE OF THE TEST SECTION.

THIS VAPOR IS GENERATED BY AN IMMERSION HEATER IN A POOL OF POTASSIUM.

③ DRY POTASSIUM VAPOR LEAVES TEST SECTION

DRY VAPOR = WET VAPOR + 5% QUALITY INCREASE

FIG 6

TEST BOILER DURING ASSEMBLY

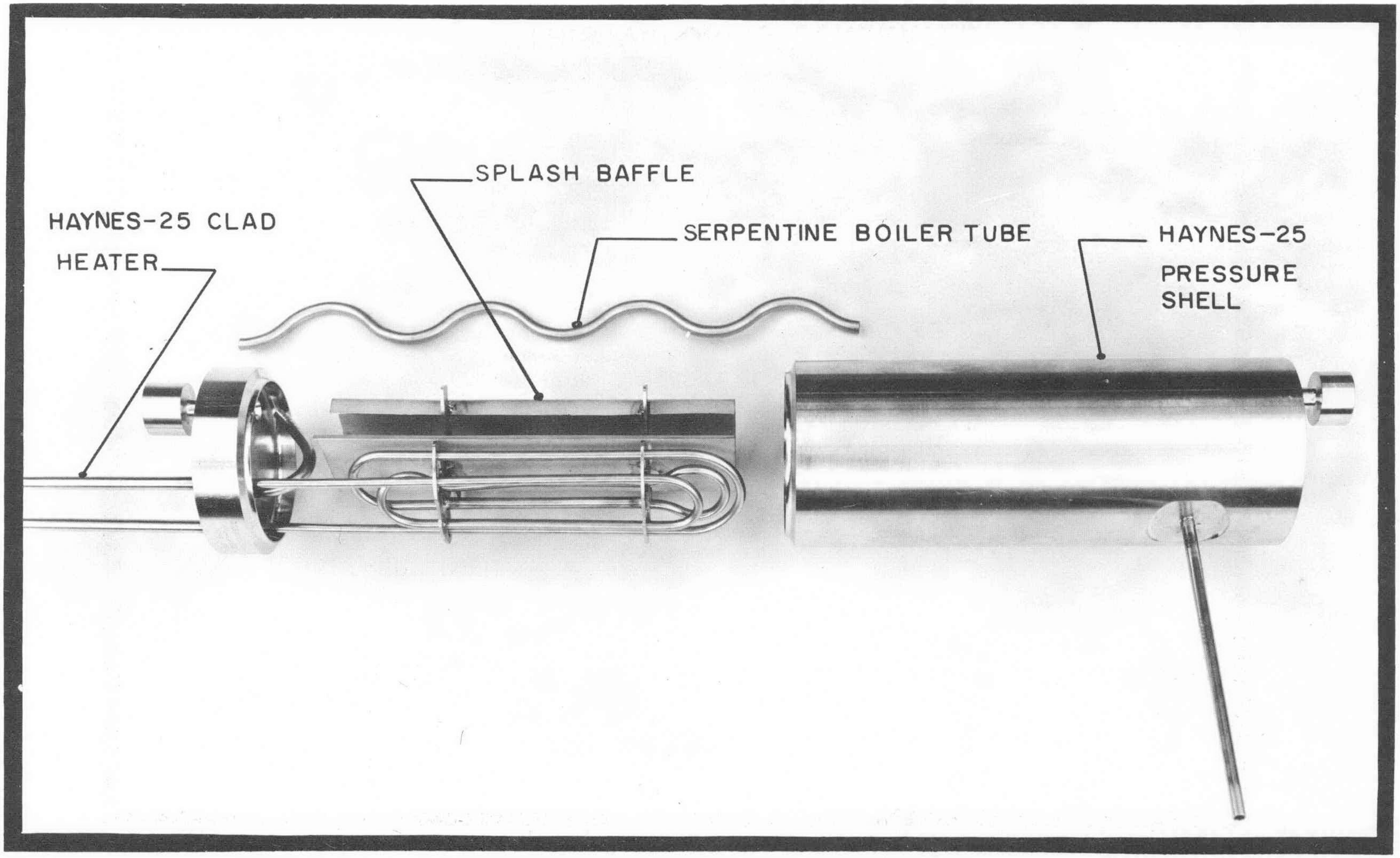

FIG 7

POST-TEST PHOTO OF TEST BOILER

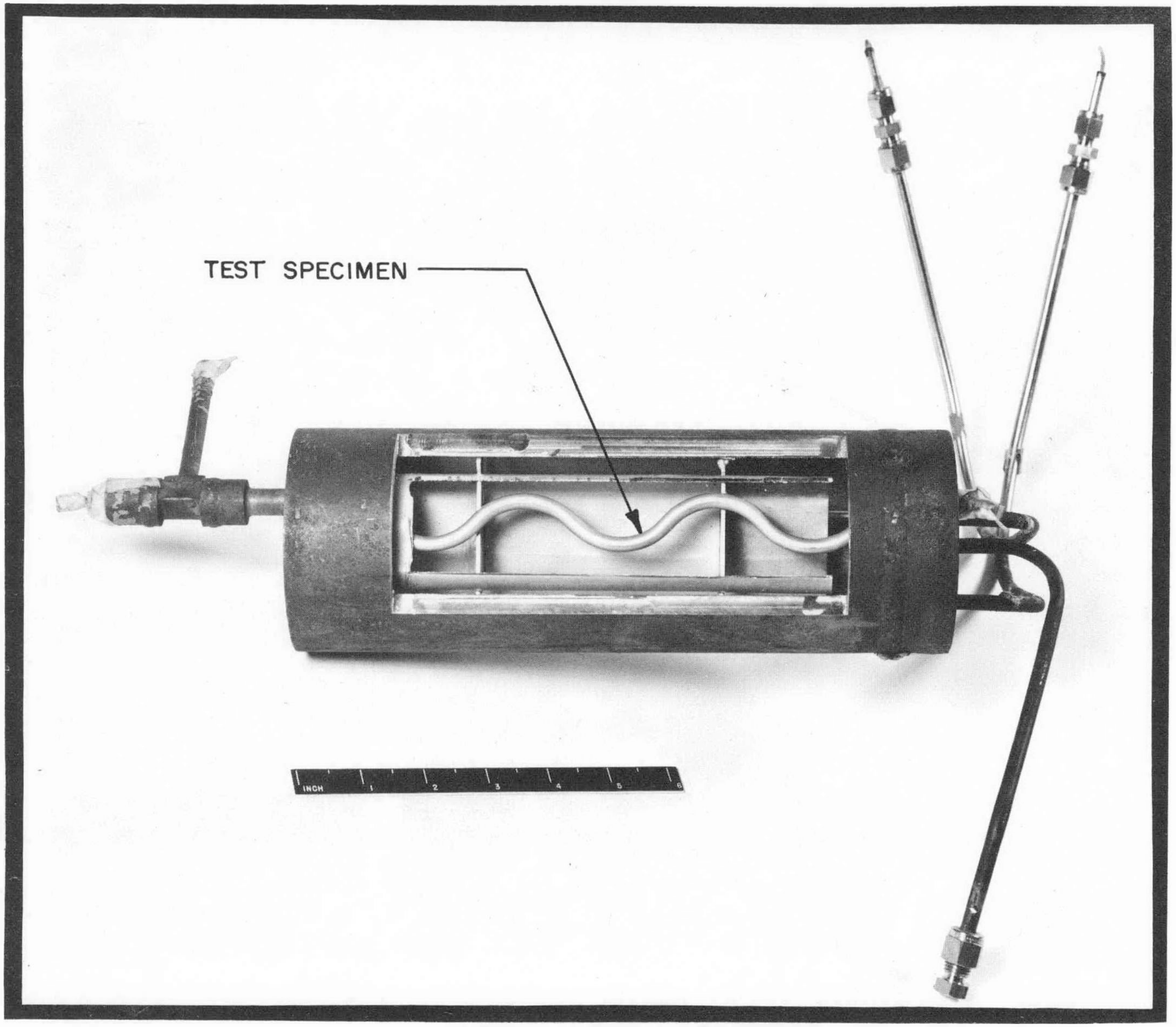

FIG 8

C13122

HAYNES-25 BOILING POTASSIUM HEAT TRANSFER LOOP

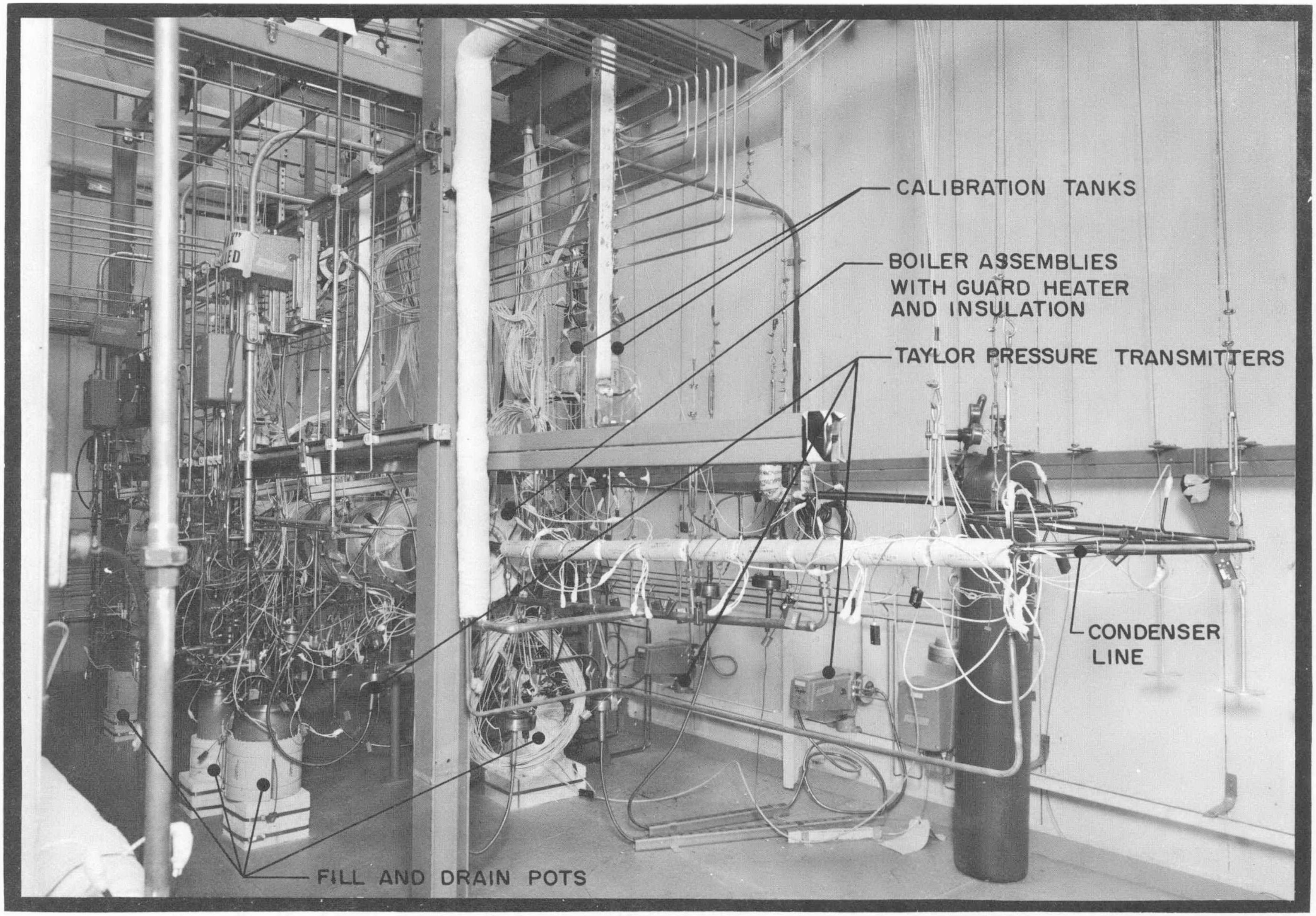

PWAC - 429

FIG 9

E-10989

CONTROL PANEL

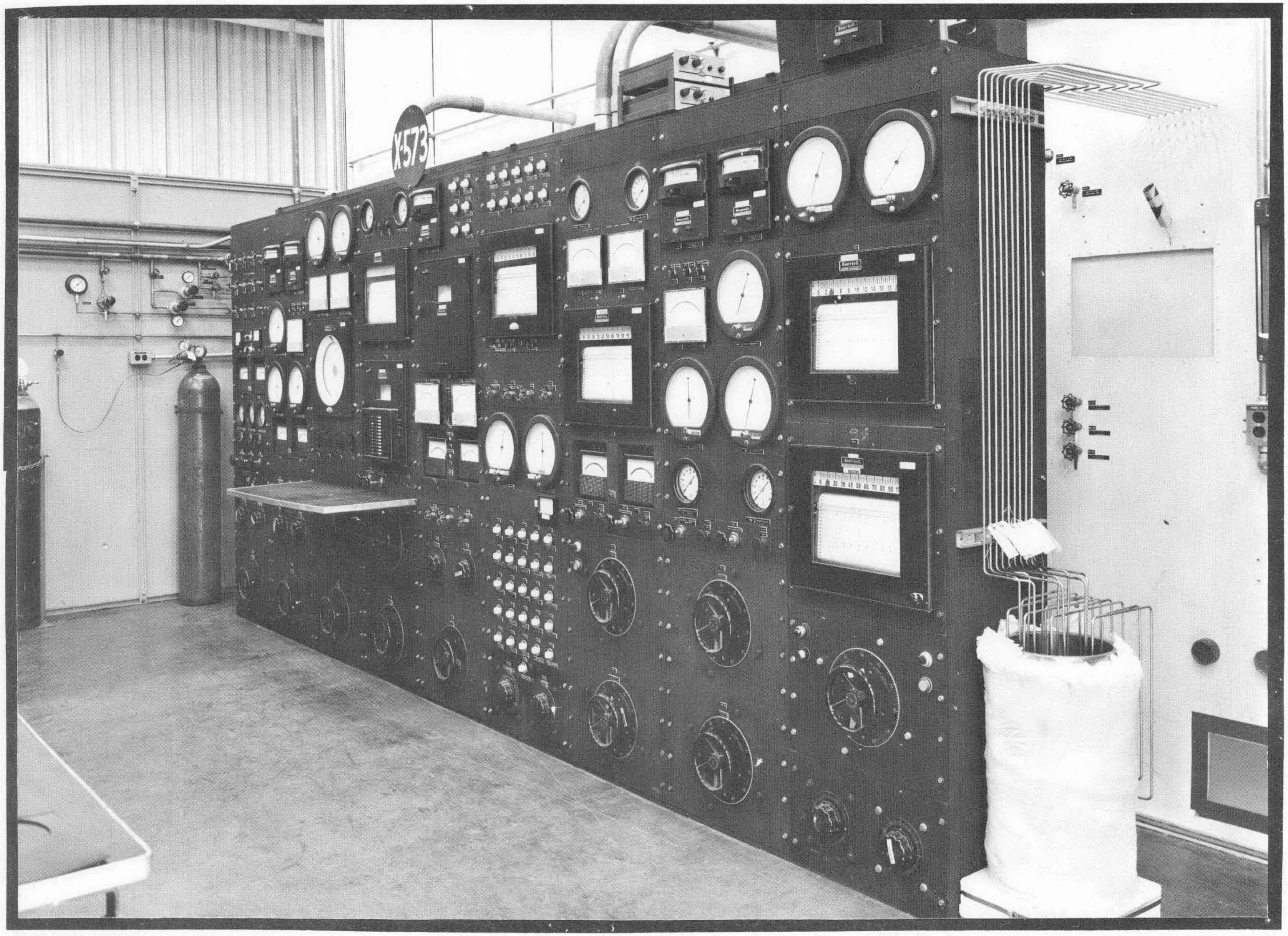

FIG 10

E-10990

III. EXPERIMENTAL EQUIPMENT

The Haynes-25 alloy heat transfer rig was designed and fabricated at Pratt & Whitney Aircraft-CANEL from a conceptual design originated at Pratt & Whitney Aircraft-East Hartford. A detailed report, CNLM-4358, entitled "Engineering Report on the Design of the Pratt & Whitney Aircraft Forced Convection Alkali Metal Vaporization-Condensation Heat Transfer Rig" which describes this apparatus, was issued, January 18, 1963. A simplified schematic is shown in Fig. 11, with a pictorial sketch of the liquid metal loop in Fig. 12. A complete schematic of the liquid metal system is included in Fig. 13. The helium cover gas schematic is shown in Fig. 14. Detailed component specifications are tabulated in Fig. 15.

A. Pump (MSA Style I)

The pump is a low-flow, alternating-current, electromagnetic type, developing high shut-off head which was useful in loop stability evaluations. The pump performance curves are shown in Fig. 16.

B. Throttle Valves (Hoke 442, Modification 1)

The manually-operated throttle valves were especially designed for high temperature liquid metal service. The spring return was replaced by a positive manual return. The throttling characteristics were good; however, two of these valves were used in series to permit fine control at low flow rates and high pressure drops.

C. Radiant Preheater

The preheater raised the temperature of the liquid potassium from 800F to 1500F. Heat was radiated from "Hevi-Duty" clamshell heaters to a concentric 3/8-inch tube. The exit temperature was measured and manually controlled with a variable transformer.

D. Preboiler (P&WA Drawing No. 1033896)

The preboiler heated the flow to saturation temperature and vaporized the fluid to any desired quality. The fluid was heated and vaporized by condensing sodium on the outside of the tube. The sodium vapor was generated by Haynes-25 clad tubular heaters immersed in a pool of sodium below the tube.

Non-condensible gases were removed by boiling the sodium and venting the vapor and gases until the pool was at the proper level. Experience in other experiments (Ref. 22) has shown that this technique removes all non-condensibles satisfactorily.

The tubular immersion heaters consisted of straight lengths of Kanthol A-1 resistance wire with nickel leads, insulated with MgO, and sheathed in 3/16-inch OD Haynes-25. The measured power factor of these heaters is unity which therefore simplified the task of measuring the power input to the boiling fluid. Heater power was manually controlled with a variable transformer.

Heat leakage was blocked by guard heaters. A pretest calibration established the power requirement of these heaters for zero heat loss (or gain) at any temperature level.

The preboiler tube is described in P&WA Drawing No. 1033897 and was identical, except for length, to the tube in the test boiler (Fig. 17).

E. Test Boiler (P&WA Drawing No. 1033898)

The test boiler accepted wet vapor from the preboiler and vaporized it to a slightly higher quality. Since the quality change is small, local heat transfer and pressure drop data is obtained.

The heating technique and heat leakage control was identical in all aspects to that described in Section III-D. The condensing fluid was potassium. The serpentine tube test section is described in P&WA Drawing No. 1033899 and pictured in Fig. 17.

Pertinent test boiler instrumentation included two differential pressure gages by which the pressure drop in the tube and the differential vapor pressure between the tube and shell were measured.

SIMPLIFIED SCHEMATIC OF HAYNES-25 BOILING POTASSIUM HEAT TRANSFER RIG

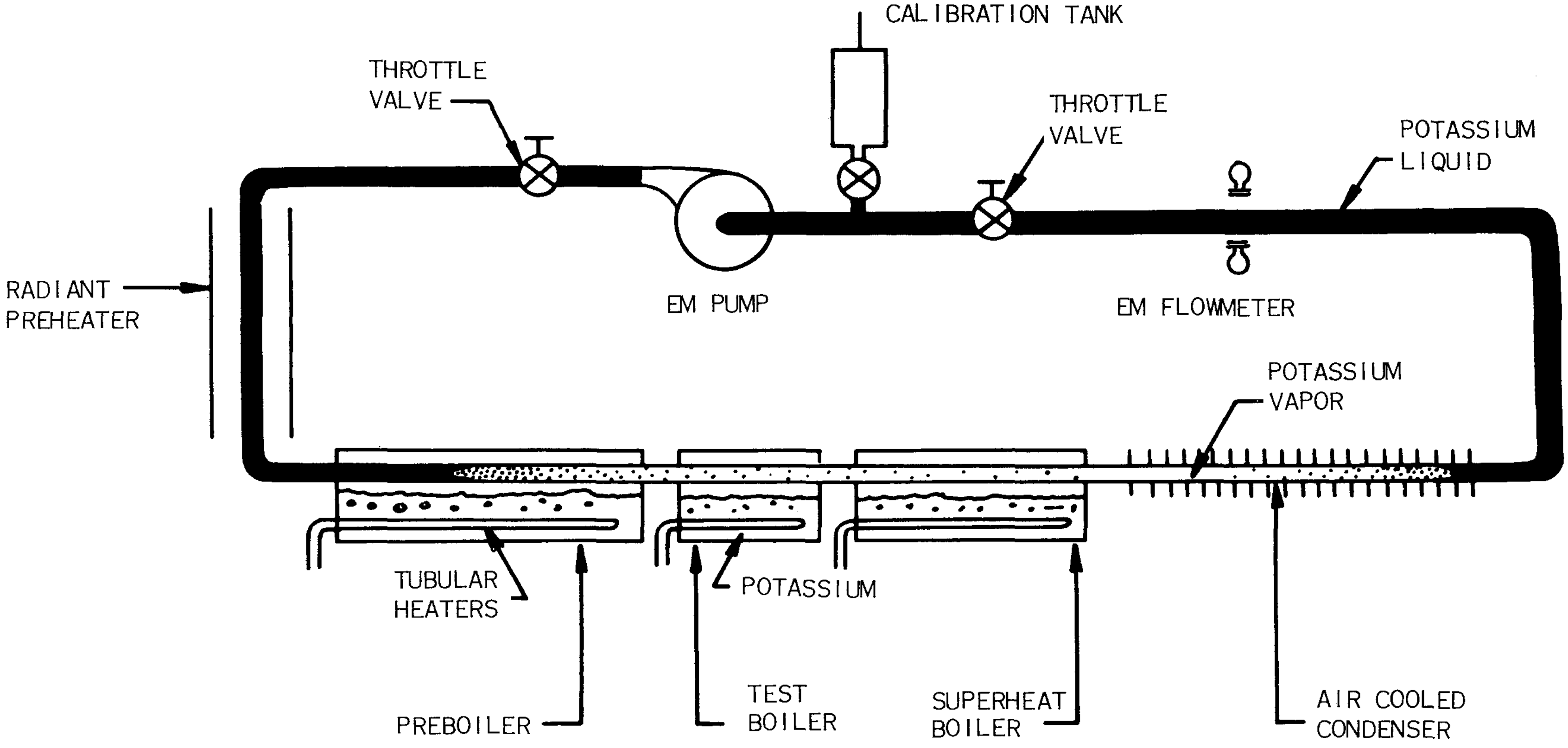

FIG 11

FIG 12

FORCED CONVECTION ALKALI METAL VAPORIZATION-CONDENSATION HEAT TRANSFER RIG

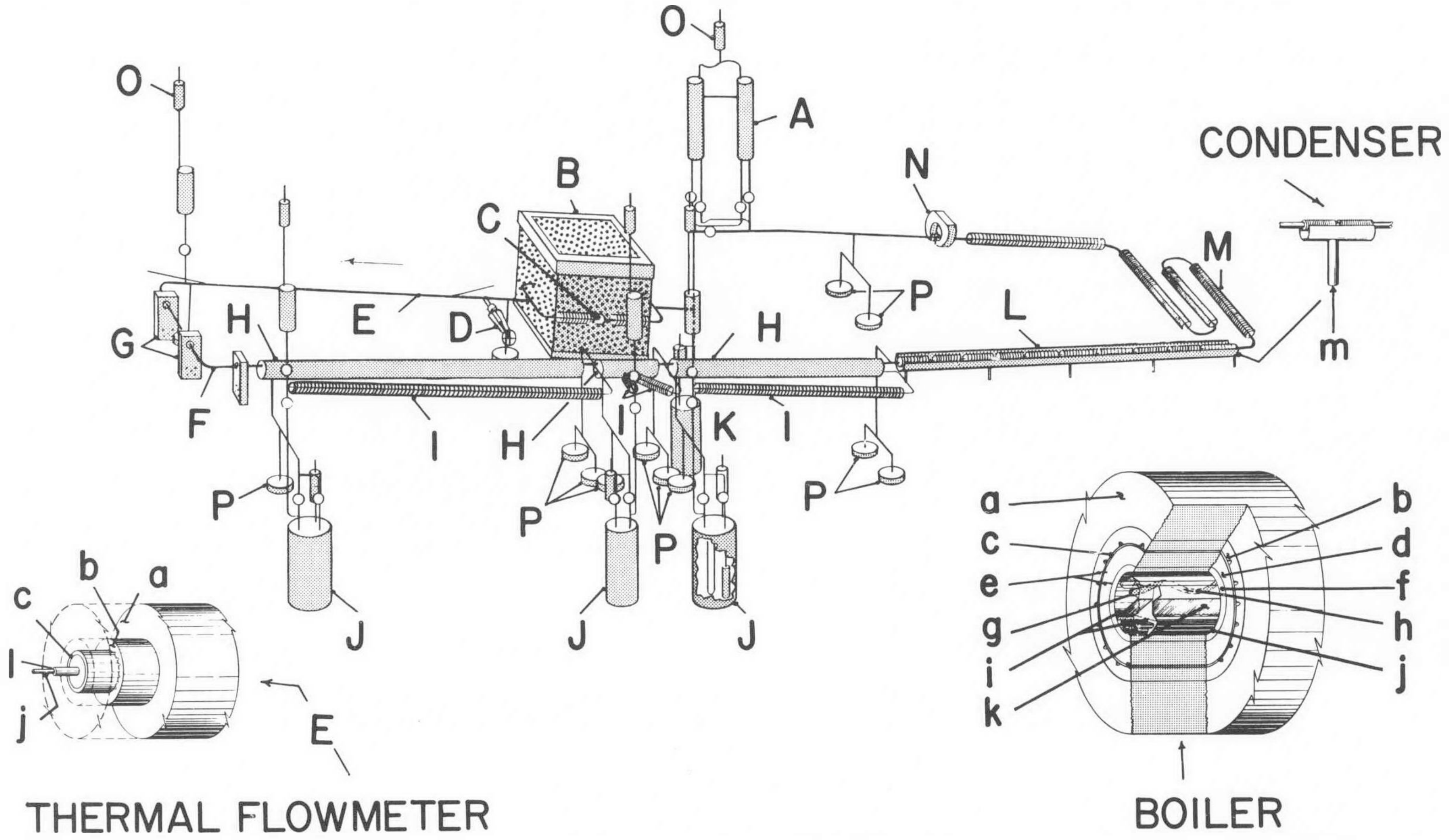

FIG 12

FORCED CONVECTION ALKALI METAL VAPORIZATION-CONDENSATION HEAT TRANSFER RIG

(CONTINUED)

A. VOLUMETRIC FLOW CALIBRATOR
B. E.M. PUMP
C. BYPASS VALVE
D. THROTTLE VALVE
E. THERMAL FLOW METER
F. RADIANT PREHEATER (LOW FLOW)
G. I^2R PREHEATER LUGS (HIGH FLOW)
H. BOILERS (3)
I. Na CONDENSER
J. Na FILL-DRAIN POT
K. POTASSIUM FILL-DRAIN POT
L. CONSTANT HEAT FLUX CONDENSER
M. NAT'L CONVECTION CONDENSER
N. E.M. FLOW METER
O. VAPOR TRAPS
P. PRESSURE TRANSMITTERS

a. INSULATION
b. CLAMSHELL HEATER
c. HEAT DISTRIBUTOR
d. INSULATION
e. THERMOCOUPLE
f. PRESSURE SHELL
g. TEST SPECIMEN
h. BOILING POTASSIUM
i. SODIUM LIQUID, SODIUM VAPOR
j. IMMERSION HEATER
k. BAFFLE
l. POTASSIUM LIQUID
m. COOLANT AIR

LOOP SCHEMATIC

LEGEND

A	E.M. PUMP	H	VAPOR TRAPS
B	PREBOILER	I	CRYOGENIC TRAPS
C	TEST BOILER	J	CONTROL PANEL
D	SUPERHEAT BOILER	K	EXPANSION TANK
E	CONDENSER	L	He BOTTLES
F	CALIBRATION TANKS	M	CALORIMETER
G	FILL AND DUMP TANKS	N	FLOW METER

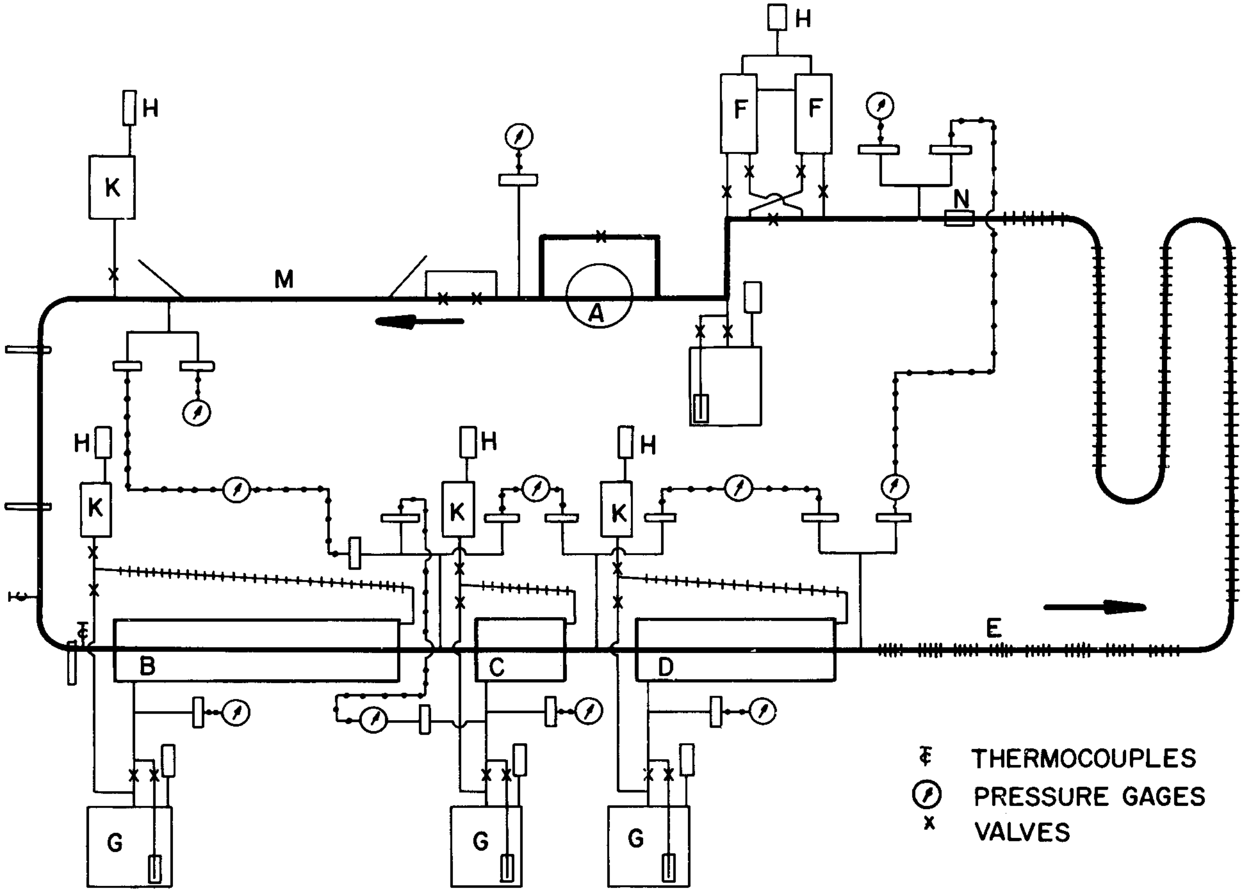

FIG 13

FIG 14

HELIUM SYSTEM SCHEMATIC

LEGEND

A	E.M. PUMP	H	VAPOR TRAPS
B	PREBOILER	I	CRYOGENIC TRAPS
C	TEST BOILER	J	CONTROL PANEL
D	SUPERHEAT BOILER	K	EXPANSION TANK
E	CONDENSER	L	He BOTTLES
F	CALIBRATION TANKS	M	CALORIMETER
G	FILL AND DUMP TANKS	N	FLOW METER

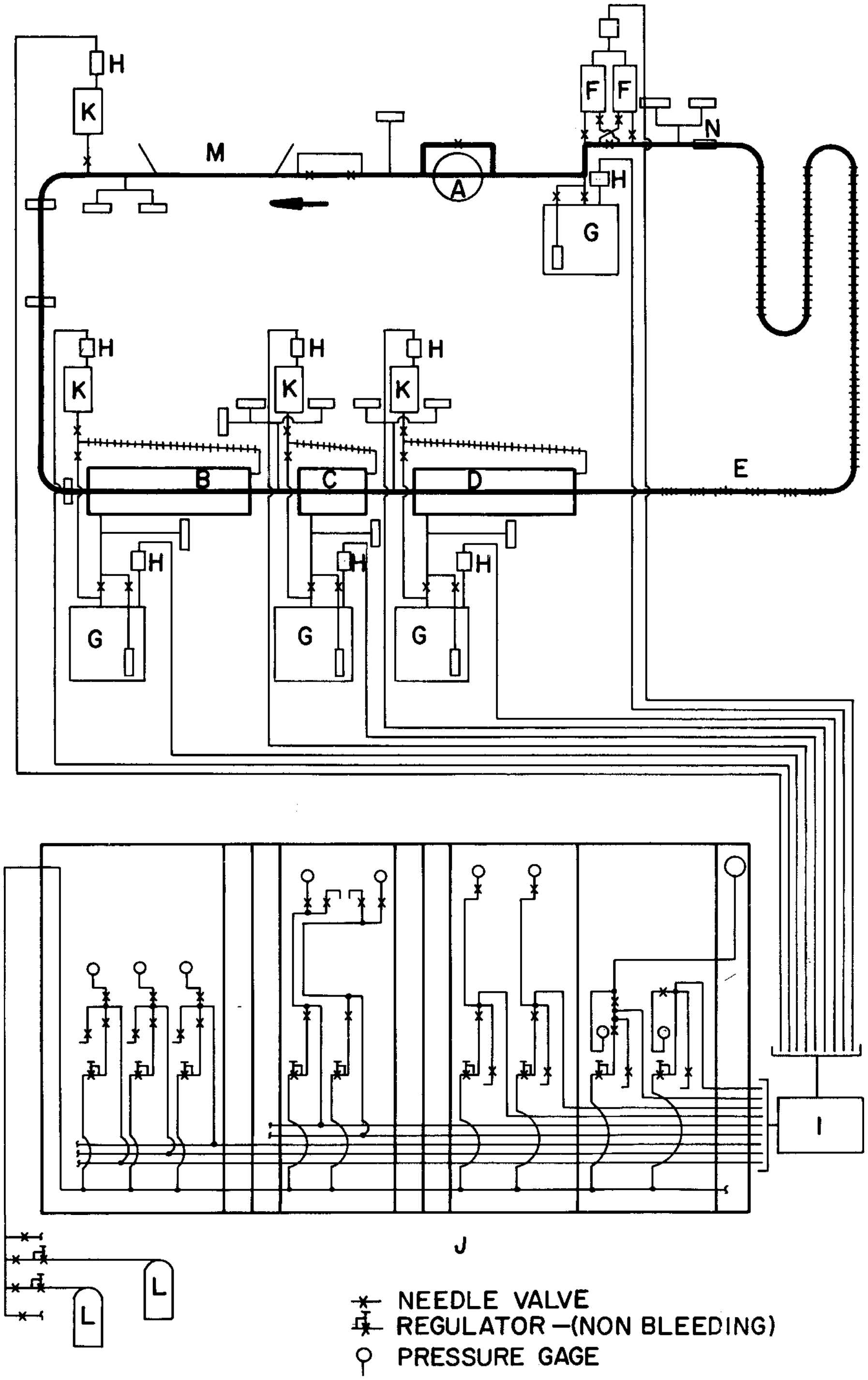

FIG 15

COMPONENT SPECIFICATIONS

(P&WA LOOP DRAWING NO. 1033925; RIG DRAWING CLR 10404)

1. Pump (P&WA Drawing No. 1033448)	
Type	Electromagnetic Conduction Pump (AC)
Manufacturer	Mine Safety Appliances Co.
Duct dimensions, in.	1/4 OD x 0.032 w
Design flow (280 volts), gpm	1.5
Design head rise (280 volts), psi	131
Shut-off head (280 volts), psi	130
Duct material	Type 316 stainless steel
2. Preboiler (P&WA Drawing No. 1033896)	
Shell OD, in.	3.5
Shell ID, in.	3.0
Tube OD, in.	0.250
Tube ID, in.	0.186
Type of boiler tube	Serpentine
Developed length of tube within shell, in.	65.5
Over-all length of tube within shell, in.	57
Design pressure (shell), psig	80
Design temperature (shell), F	1800
Design power (2-SKN 17109 heaters), Kw	9
Design time, hr	1000
Material	Haynes-25 alloy
Slope, degrees	0.5 (upward)
3. Test Boiler (P&WA Drawing No. 1033898)	
Shell OD, in.	3.5
Shell ID, in.	3.0
Tube OD, in.	0.250
Tube ID, in.	0.186
Type of boiler tube	Serpentine
Developed length of tube within shell, in.	10.35
Over-all length of tube within shell, in.	9

FIG 15

COMPONENT SPECIFICATIONS

(P&WA LOOP DRAWING NO. 1033925; RIG DRAWING CLR 10404)
(CONTINUED)

Design pressure (shell), psig	80
Design temperature (shell), F	1800
Design power (1-SKN 17110 heater), Kw	1-3
Design time, hr	1000
Material	Haynes-25 alloy
Slope, degrees	0.5 (upward)

4. Superheat Boiler (P&WA Drawing No. 1033900)

Shell OD, in.	3.5
Shell ID, in.	3.0
Tube OD, in.	0.250
Tube ID, in.	0.186
Type of boiler tube	Serpentine
Developed length of tube within shell, in.	41.4
Over-all length of tube within shell, in.	36
Design pressure (shell), psig	80
Design temperature (shell), F	1800
Design power (2-SKN 17111 heaters), Kw	5.5
Design time, hr	1000
Material	Haynes-25 alloy
Slope, degrees	0.5 (upward)

5. Vapor Traps (P&WA Drawing No. 1033150)

Type	Condensing
Diameter, in.	1.5
Length, in.	8
Loop side temperature, F	400
Gas side temperature, F	70
Internals	Wire mesh

6. Cryogenic Trap (P&WA Drawing No. CC-103701)

Cryogenic liquid	Liquid nitrogen
Filter material	Activated charcoal (CS1947)

FIG 15

COMPONENT SPECIFICATIONS

(P&WA LOOP DRAWING NO. 1033925; RIG DRAWING CLR 10404)
(CONTINUED)

7. Valves

Hoke Part No.	THY 442
Type	Needle
Orifice size, in.	5/32
Plug tip material	Stellite 6
Body material	Type 316 stainless steel
Seal	Bellows
Bellows material	Type 347 stainless steel
Pipe connection, in.	1/4 OD x 0.065 wall
Flow coefficient, Cv	0.33
P&WA part number	1033461
Hoke Part No.	HY 473 Mod 20
Type	Needle
Orifice size, in.	5/16
Plug tip material	Stellite 6
Body material	Type 316 stainless steel
Seal	Bellows
Bellows material	Type 347 stainless steel
Pipe connection, in.	3/8 OD x 0.065 wall
Flow coefficient, Cv	1.0
P&WA part number	1033418

8. Condenser (P&WA Drawing Nos. 1033452 and 1033460)

Type	Finned tube
Tube dimensions, in.	0.250 OD x 0.032 wall
Tube material	Haynes-25 alloy
Fin dimensions, in.	0.50 x 0.010 thk
Fin material	Haynes-25 alloy
Braze material	Coast Metal 52
Fins thick	30
Length, ft	14
Slope, degrees	2 (upward)

9. Potassium Loop Fill and Drain Put (P&WA Drawing No. 1033254)

LM filler porosity	5-micron
LM getter material	Titanium sponge CS-1941
Design temperature, F	1600

FIG 16

PUMP PERFORMANCE AND SYSTEM PRESSURE DROP

(MSA STYLE 0.5-150 ELECTROMAGNETIC PUMP)

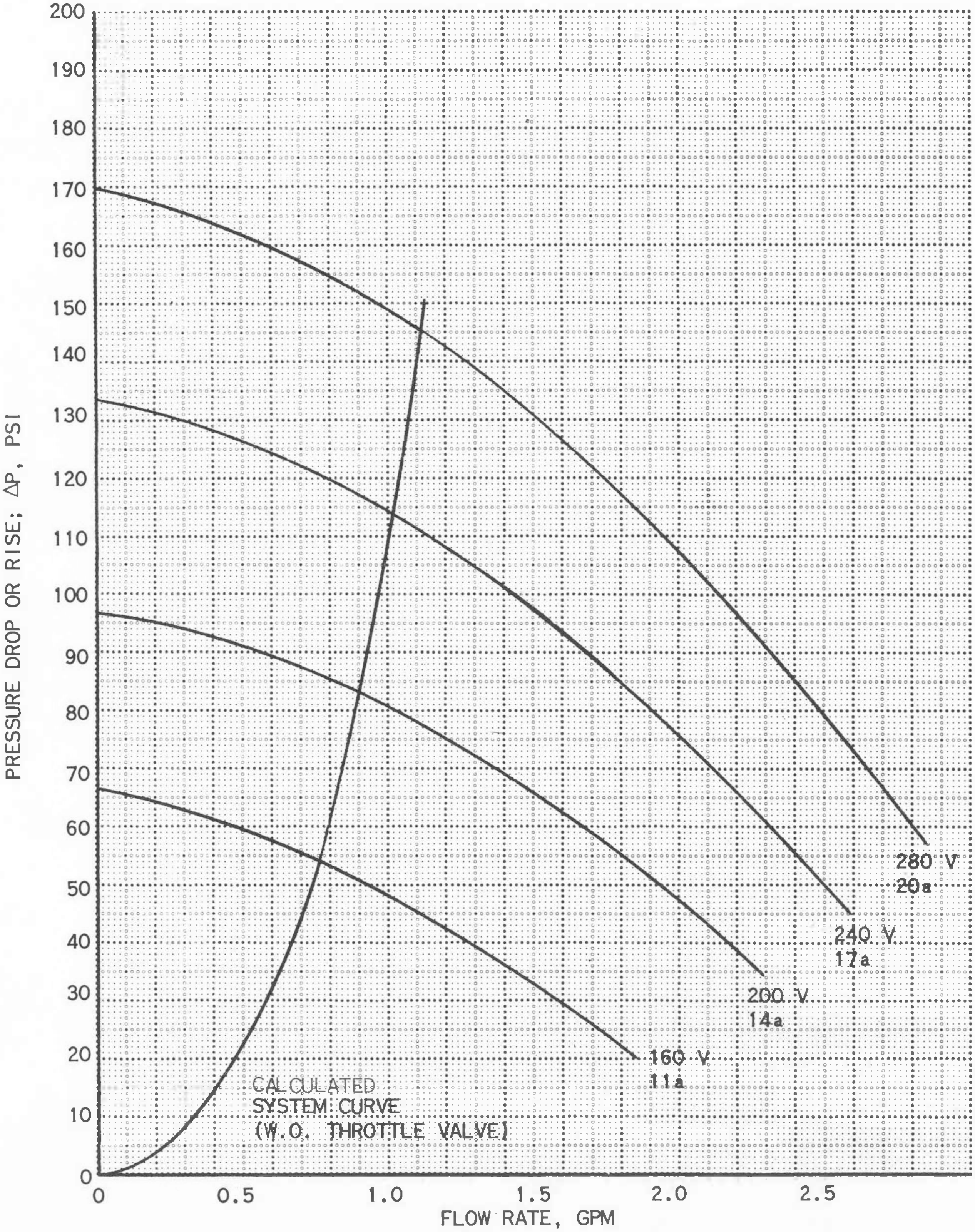

TYPICAL SERPENTINE TUBE

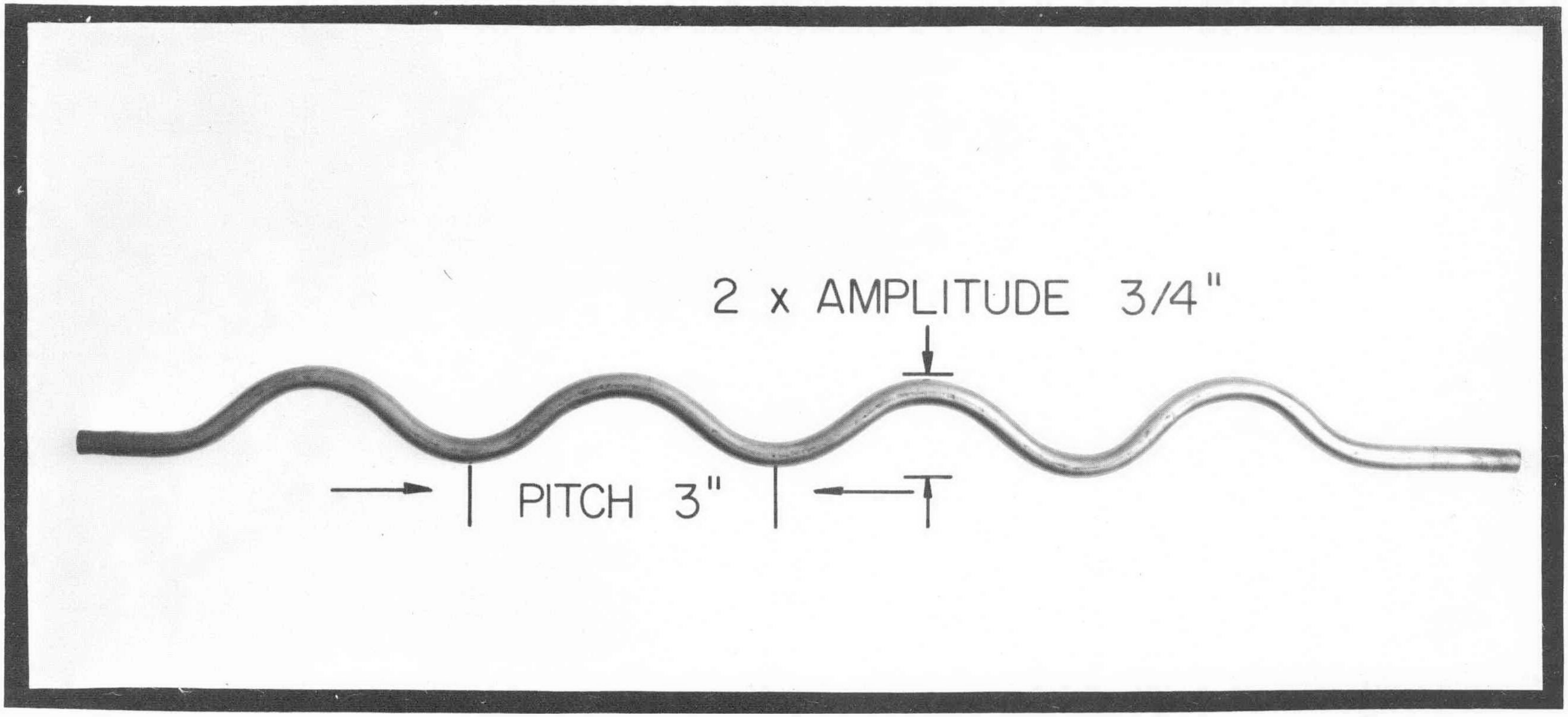

FIG 17

E-12631

The differential pressure was converted to differential temperature using the slope of the potassium vapor pressure curve at the test temperature. A differential pressure of 1.0 psi represents 4.3F at 1700F. The differential temperature obtained by this technique is considered quite accurate, since the error in the ΔP measurement is estimated at no more than 2 percent of full-scale reading, or 0.18 psi.

This technique of heating with condensing metal vapors was chosen for the following reasons:

1. Uniform wall temperature data is achieved. This type of data is directly amenable to design computations.
2. Accurate temperature differences are obtained by pressure differential measurements.
3. Simple instrumentation requirements.
4. The heat flux is precisely known and controlled.

F. Superheater (P&WA Drawing No. 1033900)

The superheater was included as a calorimetric device from which the heat balance could be checked.

This component was identical in all aspects to the preboiler except for tube length. The condensing fluid was sodium.

Unfortunately, the two thermocouples designated to measure the exact amount of superheat at the exit of this boiler failed during preheating, eliminating its usefulness as a calorimeter.

G. Condenser (P&WA Drawings No. 1033452 and 1033460)

The condenser consisted of a single finned tube (30 fins/inch) in a near horizontal attitude (2 degrees upward). The first six feet of tubing was designed for forced convection cooling. An additional eight feet of finned tubing was included for natural convection cooling. Natural convection was adequate for all tests.

H. Miscellaneous

1. Auxiliary Valves (Hoke THY-442, Modification 1, and Hoke HY-473, Modification 20).

   These manually-operated liquid metal throttle valves were especially designed for high temperature liquid metal service. The spring return was replaced by a positive return. They were all-welded, bellows-sealed needle valves.

2. Calibration Tanks (P&WA Drawing No. 1033256)

   These devices, which were connected to the loop at the pump inlet, had several functions:

   a. They served as expansion tanks during single-phase preheating.

   b. They served as an accumulator (absorb pressure and mass fluctuations) during two-phase flow operation.

   c. They served as a flowmeter calibration device. The flowmeter was volumetrically calibrated by flowing from one tank into the other through the loop. The change in liquid level was measured and the time recorded. "J" probes were used in measuring the liquid level change and a stop watch was used to measure time (Ref. Section IV-A).

IV. INSTRUMENTATION

A. Electromagnetic Flowmeter (Fig. 18)

A 2266.2-gauss permanent magnet was placed around the tube downstream from the condenser. The voltage (0.15 - 0.20 mv) generated by the flowing potassium liquid was measured. The flow rate was calculated as follows:

$$\frac{Q}{E} = \frac{\beta d_i}{3.188} \times 10^4 \times \frac{1}{R}$$

$$\frac{1}{R} = \frac{1 + (d_i/d_o)^2}{2(d_i/d_o)} + \frac{P_f}{P_w} \; \frac{1 - (d_i/d_o)^2}{2\,(d_i/d_o)}$$

d_i = inside diameter, inches

d_o = outside diameter, inches

P_f = resistivity of fluid, ohms/cm

P_w = resistivity of tube wall, ohms/cm

β = magnetic field, gauss

Q = volumetric flow rate, gallons/minute

E = electrical output, millivolts

The calculated flow rate was lower than the calibrated flow rate (Fig. 18) by approximately 10 percent. The calibration was reproducible within 1 percent. The calibrated rate was used in all calculations.

B. Differential Pressure Measurements

Differential pressure measurements were obtained by Taylor Model 225TN114 differential pressure transmitters. An accuracy of 2 percent of scale reading was assured by pretest calibrations. The vendor-quoted speed of response (63.2 percent time) was one second.

C. Pressure Measurements

Liquid metal pressures were measured by Taylor Model 225TN5114 pressure transmitters. These transmitters were checked periodically with a precision Heiss gage which was used to measure the accumulator pressure. An accuracy of 2 percent of scale reading seems reasonable based on pretest calibration (Fig. 19) and instrument checks made during the test. The vendor-quoted speed of response (63.2 percent time) was one second.

D. Electric Power Measurements

Electric power into the immersion heaters was measured by Weston Type 904-1902004 multi-range voltmeters, and Weston Type 904-2903001, 904-2903004, multi-range ammeters. An instrument accuracy of 1/2 percent of full scale was verified by pretest calibration. Since the capacitance and inductance of the immersion heaters was shown to be insignificant, the power was taken as the product of volts and amperes.

E. Liquid Level Measurements (Ref. 21)

Liquid level measurements were taken at several places, primarily to establish proper operating levels and to obtain a volume-time calibration for the flowmeter.

Two "J" probes were installed in all tanks, although only one probe was electrically connected at any time. Twenty-two probes were used in the test rig. All probes functioned well during the duration

FIG 18

ELECTROMAGNETIC FLOWMETER CALIBRATION

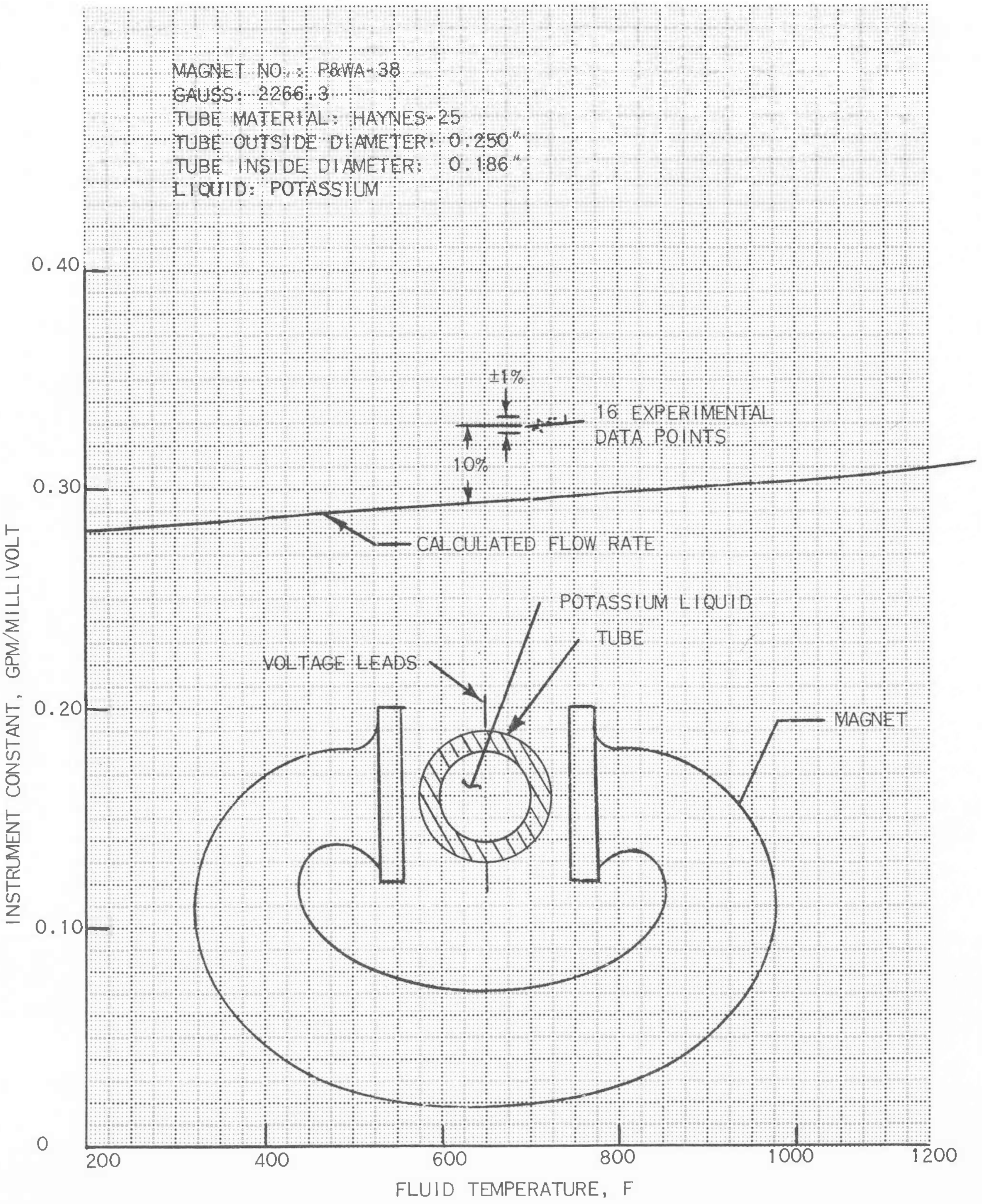

FIG 19

PRETEST PRESSURE GAGE CALIBRATION

	Pressure Gages						
Standard (psig)	5.0	10.0	15.0	20.0	30.0	40.0	50.0
PI-1	5.0	10.0	15.0	20.0	30.1	40.1	50.1
PI-2	5.0	10.2	15.2	20.25	30.6	40.7	50.9
PI-3	5.0	10.1	15.0	20.0	29.9	39.8	49.6
PI-4	5.0	10.15	15.0	20.0	30.05	40.0	49.5
PI-5	5.0	10.2	15.2	20.3	30.4	40.5	50.25
PI-6	5.0	10.0	14.9	19.95	30.1	40	49.7
PI-7*	0	0	0	0	0	0	0
PI-8*	0	0	0.1	0.1	0.2	0.2	0.2
PI-9*	0	0	0	0	0	0	0
PI-10*	0	0	0	0	0	0	0
PI-11	5	10.1	15.0	20	30	40	49.8
PI-21*	0	0	0	0	0	0	0

*Differential pressure gages at 0 psi

of the test. The "J" probes are described in P&WA Drawing No. L-101522. The levels in all except the accumulator tanks were indicated by millivolt indicators. The levels in these tanks were recorded on an oscillograph.

F. Thermocouples (P&WA Drawings No's. 1029530, 1029286, 1027164, Ref. 20).

Boiler thermocouples were Chromel/Alumel couples sheathed in 1/8-inch OD stainless steel.

Loop thermocouples were Chromel/Alumel wires tacked onto external surfaces with a condenser discharge welded, and spaced with MgO insulators.

The location of all pressure, preheater, temperature, and flow-sensing points is shown in Fig. 13.

V. EXPERIMENTAL PROCEDURES

Typically, the power into the first boiler (preboiler) was adjusted to obtain the required vapor quality at a set flow rate and pressure. The power in the second test boiler was set to obtain a desired heat flux. The test boiler was sized to minimize the quality change. The third boiler was set at a nominally low power, since a heat balance check from the superheated state was not possible because of failure of the exit thermocouples. When steady state conditions were obtained, data was recorded. Steady state operation was defined as that state when the flow, loop pressure, and differential pressure between the boiling liquid and condensing vapor was constant for more than 20 minutes.

Initially, the loop was brought to two-phase operation by lowering the pressure in the accumulator. During the life of the experiment (3625 total hours), two-phase data was taken during the day shift and the loop was operated in single-phase during the night shifts. Subsequent to the initial start, the loop converted from two-phase to single-phase operation by throttling the valve at the condenser exit and turning off the immersion heaters. Two-phase operation was initiated by reversing this procedure.

Heat loss calibrations were conducted initially and repeated periodically. The condensing resistance at the test section OD was found to be negligible.

A. Boiler Heat Loss Calibration

Zero heat leakage was maintained by external clamshell heaters placed around the boilers. The required heater power for zero heat loss was determined by recording the powerstat setting necessary to maintain a given boiler temperature with zero potassium flow and no immersion heat generation. These settings were maintained during the test to correspond to the test temperature. All heat generated by the immersion heaters was then presumed to go into the boiling process. This heat input was used, by means of a heat balance across the preboiler, to determine the vapor quality entering the test boiler; it was used in the test boiler to determine the average quality and the heat transfer coefficient.

B. Condensing Coefficients

The engineering literature indicates good agreement between Nusselt's Theory (Ref. 17) and liquid metal condensing data at low condensing rates (Reynolds Moduli). The condensing rates on the outside of the tube were quite low, and negligible condensing Δt's were anticipated. Any error in the calculated condensing coefficient was assumed to be small. This was demonstrated in preliminary tests in the nucleate boiling regime. In this regime, the boiling coefficient is very high. If the condensing resistance were significant, a high over-all Δt would result. However, for a heat flux of approximately 20,000 Btu/hr ft^2 in the test section, the overall Δt was only 5F. Assuming no boiling resistance, this represents a maximum condensing Δt of 2F. A two-degree absolute error represents a small error in the boiling coefficient in the region of most interest (high quality, low h).

The Nusselt correlation (Ref.17) indicates a 0.1F condensing Δt at a heat flux of 20,000 Btu/hr ft^2. This correlation was used in all calculations.

C. Pressure Gage Zero Shift Calibration

The over-all tube-to-shell temperature difference in the test boiler was obtained by measuring the tube-to-shell saturation pressure difference and converting the pressure difference to temperature difference using the slope of the potassium vapor pressure curve. In order to measure the tube-to-shell pressure difference as accurately as possible, it was necessary to devise a calibration technique by which the zero position of the differential pressure transmitter could be easily checked.

The calibration was performed by holding the preboiler at such temperature to only preheat the potassium to saturation conditions. Boiling was accomplished in the test boiler at some nominal heat input and flow rate. Heat loss in the test boiler was held constant at zero by proper adjustment of the guard heaters (Section V-A). The power to the test boiler immersion heater was then cut off, and the residual heat was removed through condensation on the test section until a zero temperature difference was attained between the shell vapor and tube inlet vapor. Since the same fluid was used in the shell and in the tube, the pressure differential approached zero. This was noted on the shell-to-tube pressure differential gage as it approached a constant reading when the zero temperature difference was achieved. This reading was subtracted from the gage reading obtained during a typical test run. One-half of the tube side pressure drop across the test boiler tube was added to the shell and tube inlet differential pressure reading, and the result was considered to be the actual pressure differential between shell and tube. This ΔP was converted into temperature difference using the slope of the potassium vapor pressure curve.

D. Preboiler Shell-to-Tube ΔT

The preboiler shell side sodium vapor pressure gage reading was calibrated against the potassium tube-side vapor pressure reading at various temperature levels to obtain a relative vapor pressure relationship. This calibration was used in reducing the data of the preboiler to determine over-all shell-to-tube ΔT.

The calibration was performed at a zero-heat-loss condition, with no potassium flow. A constant sodium pressure controlled by the immersion heater was maintained on the shell side of the boiler. The potassium pressure was then decreased until a volume change was noted in the calibration expansion tank "J" probe. Readings of the potassium and sodium pressures were simultaneously recorded during this inventory change. The process was repeated by pressurizing the potassium until a drop in the "J" probe level reading was noted. It was found that the volume change occurred at a potassium pressure reproducible within 0.2 psi, whether raising or lowering the pressure. Various pressure levels were similarly calibrated and the results are shown in Fig. 20. Fig. 20 is not corrected for sodium and potassium head effects and is, therefore, directly applicable to the gage readings.

FIG 20

EXPERIMENTAL RELATIONSHIP OF POTASSIUM AND SODIUM VAPOR PRESSURE

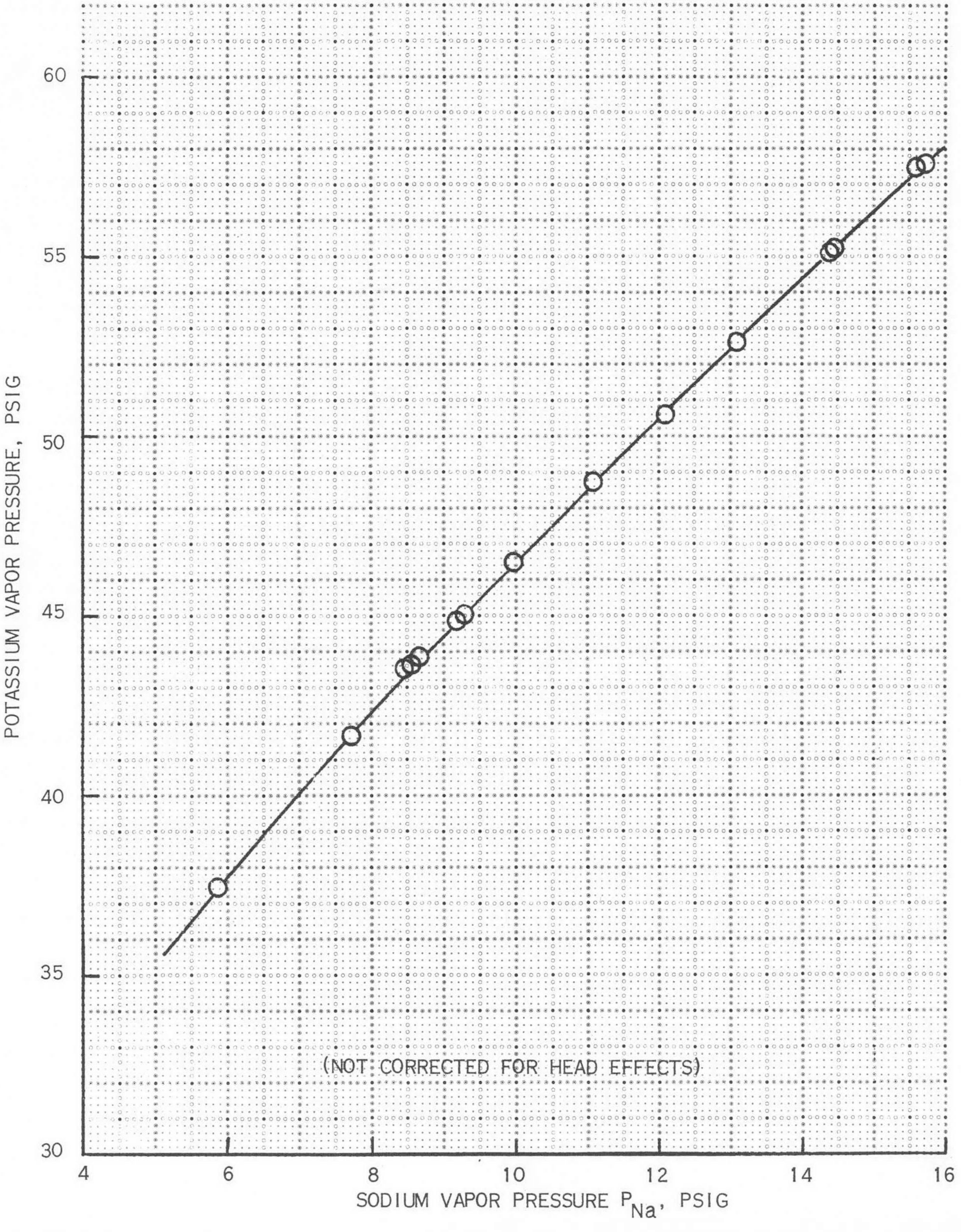

VI. EXPERIMENTAL RESULTS

A. Test Boiler Heat Transfer and Pressure Drop Data

Heat transfer and pressure drop data was obtained within the range of experimental parameters indicated in Fig. 2. The data is included in tabular form in Fig. 21 and in graphic form in Figs. 3, 4, and 22. The data was represented by the equations in Appendix A, which were used in a computer program to design the boiler shown in Fig. 5. The heat transfer data indicates the following: 1) nucleate boiling extends to about 85 percent vapor quality for this tube (Fig. 3); 2) the effect of pressure and flow is small within the ranges tested; 3) the effect of heat flux is most noticeable in the nucleate boiling regime (Fig 22); 4) the data in the film-bound regime agrees with water data in a similar tube (Fig 22); 5) the data in the nucleate boiling regime departs from water data in a similar tube (Fig. 22).

The pressure drop data shows good agreement with the Martinelli-Lockhart two-phase pressure drop correlation (Fig. 4). When the straight tube correlation is multiplied by the ratio of single-phase friction factors at the vapor Reynolds Number for straight tubes and serpentine tubes (Ref. 22) the data bounds the correlation by ± 20 percent. The pressure drop for this serpentine tube is 24 percent greater than a straight tube.

An error analysis indicates the following:

Error Analysis

	High Quality Regime	Low Quality Regime
Heat Transfer Coefficient	± 5%	± 25%
Quality	± 5%	± 10%
Pressure Drop	± 5%	± 10%

The difference is experimental error between the high quality and the low quality regimes is primarily a result of the magnitude of the pressure differentials and heat input. Fig. 23 depicts a bank of experimental uncertainty which includes the above errors, as applied to the "h versus x" plots.

B. Preboiler Heat Transfer and Pressure Drop Data

The over-all data for this boiler is included in Figs. 21 and 24.

The over-all heat transfer data indicates a slight decrease for qualities greater than 85% vapor quality. This is consistent with the performance in the test boiler. A calculated U for the preboiler using local data from the test boiler agrees with the experimental U within 10 percent.

Observations of the shell side pressure during boiling initiation indicated that approximately 50F to 70F liquid superheat was required to initiate boiling. This was indicated by the following sequence of events:

1. Power into the preboiler was turned on with single-phase liquid flowing in the tube. A small (~1 psi) tube pressure drop was indicated.
2. The pressure in the shell rose and continued to rise a significant amount. The tube pressure drop was still small.
3. The tube side pressure drop rose a significant amount (5 psi) and the shell side pressure dropped. The increase in tube side pressure drop indicated initiation of boiling.

FIG 21

EXPEREMENTAL DATA

Date	Run No.	Condenser-Discharge Static Pressure (psia)	Preboiler Tube-Side Pressure Drop (psi)	Test Boiler Tube-Side Pressure Drop (psi)	Mass Flow Rate (lb/hr)	Preboiler Boiling Heat Flux (Btu/hr-ft^2)	Test Boiler Boiling Heat Flux (Btu/hr-ft^2)	Preboiler Subcool ΔT, (F)	Preboiler Heat Into Preheat (Btu/hr)	Preboiler Heat Into Boiling (Btu/hr)
7/2/63	1	49.55	4.053	1.55	18.9	53, 600	4, 230	248.0	885	13, 500
	2	48.84	3.817	1.464	16.4	48, 900	4, 230	194.7	606	12, 500
	3	45.92	4.47	1.73	17.4	54, 500	17, 180	159.3	529	14, 170
	4	48.11	3.98	1.63	17.4	50, 700	17, 560	127.8	427	13, 173
	5	47.81	3.91	1.578	16.9	50, 700	17, 560	119.7	390	13, 210
	6	48.21	3.93	1.60	17.3	50, 700	17, 560	119.2	397	13, 200
	7	48.20	3.93	1.61	17.0	50, 700	17, 560	114.2	374	13, 225
	8	48.19	3.95	1.588	16.5	51, 800	17, 560	222.2	693	13, 157
	9	48.20	4.0	1.616	17.9	52, 700	17, 400	216.0	732	13, 388
	10	48.86	4.043	1.68	18.15	53, 100	17, 180	213.0	732	13, 388
	11	48.76	4.13	1.708	18.03	52, 900	17, 180	228.0	779	13, 381
7/3/63	12	48.56	4.218	1.68	17.65	59, 300	17, 110	237.5	791	15, 100
	13	48.36	3.87	1.61	17.65	51, 000	17, 110	222.5	744	12, 906
	14	48.16	3.835	1.578	17.4	51, 000	17, 110	221.5	730	12, 920
	15	48.46	3.80	1.58	15.9	51, 000	16, 570	225.0	679	12, 971
	16	48.56	3.91	1.58	17.0	52, 700	16, 570	230.7	743	13, 350
	17	48.66	3.945	1.57	16.9	52, 400	16, 570	228.0	729	13, 320
	18	48.65	3.98	1.58	17.14	53, 000	16, 570	225.2	731	13, 470
	19	48.84	4.11	1.64	17.32	50, 200	16, 570	225.1	738	12, 610
	20	48.74	4.00	1.61	17.4	53, 700	16, 570	225.3	741	13, 660
	21	53.34	3.62	1.55	17.27	51, 800	18, 000	200.0	657	13, 220
	22	53.36	3.60	1.52	17.0	51, 800	18, 000	198.3	641	13, 240
	23	53.36	3.60	1.53	17.14	51, 800	18, 000	198.3	647	13, 233
	24	55.27	3.59	1.45	16.76	50, 200	16, 950	216.8	690	12, 760
7/8/63	25	56.01	0.19	0.0469	17.26	4, 488	17, 087	278.2	899	305
	26	56.61	0.19	0.0505	16.63	4, 488	17, 337	251.2	785	419
	27	57.01	0.19	0.0505	16.63	2, 507	17, 337	246.8	772	0
	28	55.41	0.19	0	14.49	2, 976	0	240.3	656	143
7/9/63	29	51.25	3.49	1.66	15.88	45, 242	11, 099	188.8	571	11, 569
	30	51.05	3.48	1.62	19.15	45, 678	17, 007	170.0	622	11, 634
	31	49.65	3.82	1.90	20.4	47, 827	16, 926	160.0	626	12, 207
	32	53.91	0.19	0.029	17.77	2, 840	677	239	798	0
	33	52.81	0.19	0	15.75	2, 840	677	268	790	0
	34	53.71	0.19	0	16.38	2, 840	677	270	828	0
	35	54.31	0.19	0	17.01	2, 840	677	255	814	0
	36	55.11	0.19	0	17.01	2, 840	677	259	826	0
	37	53.81	0.19	0	17.51	2, 840	677	257	844	0
	38	53.71	0.19	0	17.64	2, 840	677	252	834	0
	39	54.36	0.19	0	16.76	2, 840	677	255	803	0
	40	54.36	0.19	0	16.76	2, 840	6, 770	255	803	0
	41	53.31	0.19	0	15.75	2, 840	6, 770	250	740	22
7/11/63	42	52.17	0.244	0	23.94	1, 990	0	313	1395	0
	43	49.88	4.20	1.89	20.16	54, 537	17, 087	172	663	13, 970
	44	49.78	4.14	1.90	19.53	54, 319	17, 087	173	646	13, 929
	45	49.88	4.32	1.92	19.78	56, 763	21, 448	174	658	14, 572
	46	50.08	4.25	1.85	19.78	56, 540	17, 256	168	636	14, 535
	47	48.56	4.03	1.805	19.03	50, 791	15, 596	163	594	13, 034
	48	49.76	4.02	1.77	18.77	51, 001	15, 596	161	578	13, 106
7/12/63	49	54.29	0.19	0.032	17.64	1, 408.1	17, 764	184	615	0
	50	54.49	0.19	0.087	18.02	1, 631.3	34, 336	175	598	0
	51	55.39	0.19	0.022	18.27	1, 755.4	17, 426	148	515	0
	52	55.79	0.19	0.020	18.52	1, 688.6	17, 176	141	498	0
	53	52.19	3.55	1.393	16.63	48, 781	8, 350	174	552	0
7/17/63	54	55.77	0.19	0.0469	17.65	2, 360	27, 800	168	562	0
	55	57.35	0.19	0.0325	17.0	1, 435	27, 600	180	581	0
	56	56.05	0.19	0.0227	17.0	1, 855	27, 600	176	569	0
7/18/63	57	53.84	1.092	0.874	17.65	22, 400	28, 000	153	515	5, 495
	58	54.72	3.29	1.60	17.75	45, 300	28, 300	243	816	11, 334
	59	55.32	3.22	1.56	17.75	47, 200	28, 400	246	826	11, 824
	60	55.32	3.37	1.61	17.40	49, 000	28, 400	252	828	12, 302
	61	55.12	3.37	1.59	17.40	49, 100	28, 500	257	843	12, 307
	62	54.91	3.44	1.64	17.0	49, 400	28, 500	253	812	12, 438
	63	54.71	3.37	1.59	17.0	49, 300	28, 500	253	812	12, 388
	64	55.51	3.04	1.46	16.65	46, 300	28, 400	249	783	11, 647
	65	56.21	3.00	1.40	16.65	46, 100	28, 500	251	790	11, 560
7/23/63	66	57.17	0.948	0.787	16.75	23, 000	28, 800	225	712	5, 468
	67	57.27	0.966	0.733	16.90	23, 100	16, 900	224	716	5, 488
7/22/63	68	56.02	0.19	0.141	17.65	1, 755	39, 400	196	656	0
	69	56.52	0.19	0.123	17.40	1, 532	39, 100	203	670	0
7/23/63	70	56.77	1.02	0.884	16.75	22, 950	39, 100	225	714	5, 436
	71	56.97	0.984	0.845	17.00	23, 000	39, 100	225	724	5, 456
	72	56.17	2.236	1.155	16.75	29, 100	38, 400	221	702	7, 098
	73	54.39	3.071	1.61	17.40	46, 600	38, 600	238	784	11, 716
	74	54.72	3.251	1.668	17.75	47, 900	38, 700	249	835	12, 015
	75	54.25	3.281	1.66	17.40	49, 250	38, 700	251	825	12, 375
7/24/63	76	55.18	1.265	1.097	18.25	27, 400	39, 800	228	787	6, 553
	77	56.18	0.948	0.938	17.00	28, 200	39, 800	207	666	6, 894
	78	56.58	3.251	1.075	17.00	25, 900	39, 800	237	762	6, 178
	79	55.97	2.751	1.25	17.25	32, 150	39, 800	232	758	7, 862
	80	55.97	3.251	1.54	17.25	45, 400	41, 000	231	755	11, 445

(See last page of this figure for footnotes)

FIG 21

EXPEREMENTAL DATA

CONTINUED

Run No.	Preboiler Exit Quality	Preboiler Average Tube to Shell ΔT (F)	Preboiler Over-all Heat Trans. Coefficient (Btu/hr-ft^2 F)	Test Boiler Tube to Shell ΔT(e) (F)	Test Boiler Boiling ΔT(e) (F)	Test Boiler Local Heat Trans. Coeff.(e) (Btu/hr-ft^2 F)	Test Boiler Boiling ΔT(f) (F)	Test Boiler Local Heat Trans. Coeff.(f) (Btu/hr-ft^2 F)	Test Boiler Average Quality	Average Tube-Side Pressure in Test Boiler, psia
1	87.8	38.6	1389	23.0	22.3	189.7	22.6	187.2	90.8	58.43
2	93.3	42.7	1145	54.5	53.8	78.6	c	--	94.0	57.06
3	99.8	46.4	1175	61.5	59.0	291.2	c	--	100.4	55.76
4	92.8	32.4	1565	39.5	36.9	475.9	30.55	574.8	95.3	57.31
5	95.9	34.8	1457	60.0	57.4	305.9	c	--	98.6	56.62
6	93.7	33	1536	66.0	63.4	277.0	c	--	96.35	57.23
7	95.5	33.8	1500	70.5	67.9	258.6	c	--	98.2	57.22
8	97.9	44.1	1175	78.0	75.4	232.9	c	--	100.67	56.98
9	91.7	51.1	1031	79.5	76.95	226.1	c	--	94.12	56.88
10	90.5	40	1328	78.0	75.5	227.5	25.40	676.4	93.0	57.81
11	91.1	33	1603	23.0	20.5	838.0	c	--	93.57	58.28
12	104.8	38	1561	b	--	--	b	--	100+	58.13
13	89.8	32.5	1569	53.0	50.5	338.8	c	--	92.3	57.37
14	91.2	33.5	1522	39.0	36.5	468.8	c	--	93.76	57.16
15	100.0	31.5	1619	42.5	40.05	413.7	c	--	102.7	57.31
16	96.5	35.7	1476	56.5	54.05	306.6	c	--	99.0	57.38
17	97.0	39.1	1340	36.5	34.05	486.6	c	--	99.5	57.38
18	96.4	39.1	1355	61.0	58.55	283.0	c	--	98.9	57.41
19	89.6	48.2	1041	65.5	63.05	262.8	c	--	92.1	57.92
20	96.4	20	2685	43.5	41.05	403.7	c	--	98.9	57.88
21	94.3	33.2	1560	30.8	28.15	636.0	32.04	561.8	97.0	61.92
22	95.9	28.4	1824	39.8	37.15	484.5	c	--	98.65	61.82
23	95.1	28.7	1805	43.3	40.65	442.8	c	--	97.83	61.82
24	93.7	27.2	1846	g	--	--	6.23	2,721	96.35	63.18
25	2.16	15.8	a	g	--	--	3.31	5,162	4.725	56.57
26	3.08	21.6	a	g	--	--	3.27	5,302	5.78	56.74
27	0	18.2	a	g	--	--	3.27	5,302	2.70	57.56
28	1.21	11.9	a	g	--	--	--	--	--	58.77
29	89.72	21.2	2134	g	--	--	3.00	3,700	91.54	61.47
30	74.82	22.7	2012	g	--	--	3.49	4,873	77.135	61.53
31	73.79	24.2	1976	g	--	--	3.97	4,263	79.955	63.45
32	0	a	--	--	--	--	2.42	280	0.0985	54.66
33	0	a	--	--	--	--	2.63	257	0.1115	53.98
34	0	a	--	--	--	--	2.27	298	0.107	54.87
35	0	a	--	--	--	--	2.16	313	0.103	55.99
36	0	a	--	--	--	--	0.27	2,489	0.1035	56.71
37	0	a	--	--	--	--	2.43	278	0.100	56.31
38	0	a	--	--	--	--	2.43	278	0.0995	56.25
39	0	a	--	--	--	--	1.77	382	0.1045	57.57
40	0	a	--	--	--	--	1.47	4,612	1.045	57.56
41	0.171	a	--	--	--	--	1.47	4,612	1.286	57.29
42	0	a	--	--	--	--	--	--	--	53.45
43	85.34	27	2020	g	--	--	3.79	4,304	87.55	61.88
44	87.84	27	2012	60.0	57.4	298	4.14	5,181	90.12	61.68
45	90.73	26	2183	--	--	--	36.32	475.1	93.56	61.79
46	90.50	27	2094	60.0	57.4	301	c	--	92.78	61.59
47	84.35	21	2419	63.0	60.64	257.2	3.81	4,093	86.49	59.85
48	85.99	26	1962	59.0	56.64	275.4	4.21	3,705	88.16	60.83
49	0	a	--	28.5	25.82	688.0	c	--	2.605	55.63
50	0	a	--	36.5	31.42	1,093	c	--	49.38	56.23
51	0	a	--	39.0	36.37	479.1	3.86	4,515	2.47	56.46
52	0	a	--	36.0	33.41	514.1	3.58	4,798	2.405	56.83
53	0	a	--	61.0	59.69	139.9	c	--	1.31	60.31
54	0	a	--	--	--	--	1.85	15,000	4.08	57.62
55	0	a	--	--	--	--	1.87	14,800	4.23	59.03
56	0	a	--	--	--	--	1.56	17,700	4.23	58.13
57	38.1	46	487	--	--	--	0.88	31,800	42.23	58.30
58	78.6	24	1888	--	--	--	1.21	23,400	82.76	63.13
59	81.9	24	1967	--	--	--	1.72	16,500	86.08	63.44
60	87.0	27	1815	--	--	--	2.73	10,400	91.26	63.86
61	87.0	26	1888	--	--	--	18.77	1,520	91.28	63.46
62	90.3	30	1647	--	--	--	34.77	821	94.68	63.31
63	89.5	34	1450	--	--	--	34.67	823	93.87	63.08
64	86.1	30	1543	--	--	--	17.08	1,665	90.55	62.53
65	85.9	27	1707	--	--	--	35.27	807	90.37	63.02
66	40.1	30	766.7	--	--	--	0.84	34,300	44.74	61.24
67	39.9	31	745.2	--	--	--	0.70	24,150	42.51	60.94
68	0	a	--	--	--	--	2.59	15,200	5.8	61.50
69	0	a	--	--	--	--	1.90	20,600	5.85	61.79
70	39.9	31	740.3	--	--	--	0.93	42,100	46.0	61.12
71	39.4	30	766.7	--	--	--	0.85	46,000	45.88	61.14
72	52.1	32	909.4	--	--	--	1.53	25,100	58.08	61.21
73	83	30	1553	--	--	--	12.80	3,010	88.78	62.71
74	83.5	26	1842	--	--	--	3.47	11,150	89.18	63.75
75	87.6	26	1894	--	--	--	60.5	635	93.4	62.95
76	44.3	35	782.9	--	--	--	1.17	34,000	49.98	61.61
77	49.7	58	486.2	--	--	--	1.91	20,850	53.9	61.81
78	44.4	8	3238	--	--	--	1.43	27,800	50.5	62.68
79	56.1	13	2473	--	--	--	1.53	26,000	58.15	62.96
80	81.8	25	1816	--	--	--	6.75	6,070	88.0	64.09

(See last page of this figure for footnotes)

FIG 21

EXPEREMENTAL DATA

CONTINUED

Date	Run No.	Condenser-Discharge Static Pressure (psia)	Preboiler Tube-Side Pressure Drop (psi)	Test Boiler Tube-Side Pressure Drop (psi)	Mass Flow Rate (lb/hr)	Preboiler Boiling Heat Flux (Btu/hr-ft2)	Test Boiler Boiling Heat Flux (Btu/hr-ft^2)	Preboiler Subcool ΔT, (F)	Preboiler Heat Into Preheat (Btu/hr)	Preboiler Heat Into Boiling (Btu/hr)
7/26/63	81	54.72	3.285	1.625	17.14	27,200	52,600	220	716	11,083
	82	54.42	3.267	1.79	17.26	33,600	52,700	226	740	11,672
7/29/63	83	56.99	0.19	0.130	17.39	6,550	51,300	203	669	1,084
	84	57.98	0.19	0.1083	17.51	1,755	51,800	202	671	0
7/31/63	85	58.18	0.19	0.00721	17.64	2,050	16,750	219	730	0
	86	56.37	0.19	0.0433	17.77	2,025	28,000	208	699	0
	87	57.37	0.19	0.0758	17.01	2,025	39,800	213	685	0
	88	58.06	0.19	0.1083	16.76	1,725	51,500	218	691	0
8/2/63	89	53.87	3.51	1.75	17.51	50,371	43,443	251	830	12,674
8/5/63	90	55.78	3.31	1.49	17.26	43,070	33,207	191	630	10,916
	91	53.58	3.98	1.68	17.26	43,070	33,207	204	669	10,877
	92	57.17	3.44	1.35	17.64	40,882	31,676	236	789	10,171
8/6/63	93	57.04	3.26	1.23	16.63	50,371	4,103	233	735	12,769
	94	52.65	4.11	1.65	18.27	54,696	4,103	241	834	13,829
	95	51.46	4.23	1.61	17.89	57,316	6,964	252	851	14,514
8/7/63	96	59.87	3.04	1.20	17.01	46,517	4,272	246	792	11,678
	97	52.26	2.97	1.32	17.64	38,465	4,272	217	725	9,587
8/8/63	98	42.84	2.93	1.47	17.67	43,070	16,604	235	785	10,761
	99	53.93	2.90	1.29	17.26	42,396	12,090	234	764	10,602
	100	55.0	2.83	1.34	17.01	42,396	24,019	239	769	10,597
	101	55.0	2.86	1.39	16.63	42,396	32,240	240	755	10,611
8/9/63	102	51.29	3.62	2.31	25.83	46,377	31,998	296	1441	10,992
	103	54.47	3.22	1.93	25.2	42,266	23,777	222	1068	10,260
	104	55.05	3.55	1.97	25.2	42,266	16,537	230	1104	10,224
8/10/63	105	51.69	4.12	1.88	20.79	50,676	11,284	203	803.9	12,781
	106	51.51	4.12	1.92	20.79	50,676	16,587	203	803.9	12,781
	107	51.61	4.14	1.98	20.79	50,676	23,938	195	774	12,811
8/11/63	108	52.45	3.87	1.98	20.79	50,676	32,562	235	928	12,657
	109	52.35	4.88	2.07	20.16	59,199	32,699	227	869	15,001
8/12/63	110	4.53	3.26	1.88	24.57	42,116	16,587	246	1145	10,146
	111	56.13	3.51	1.98	24.57	45,092	16,990	257	1197	10,891
	112	53.93	3.22	1.85	24.57	38,783	16,741	246	1145	9,252
	113	53.53	2.97	1.70	24.82	35,591	16,741	240	1129	8,412
	114	52.73	2.79	1.57	24.28	32,411	16,741	235	1081	7,607
8/13/63	115	51.41	2.48	1.44	24.57	32,690	1,752	212	988	7,783
	116	51.21	2.59	1.48	24.57	32,818	1,699	202	943	7,862
	117	57.38	2.0	1.12	25.20	26,076	16,749	209	998	5,999
8/14/63	118	52.24	3.62	2.04	24.82	45,169	6,587	235	1106	11,013
	119	51.84	3.98	2.21	24.82	48,272	16,749	227	1070	11,882
	120	51.67	4.16	2.31	24.82	48,272	16,749	216	1021	11,931
	121	52.99	5.44	2.35	25.20	51,567	16,749	235	893	12,943
	122	51.10	4.70	2.47	25.20	54,696	16,749	240	912	13,764
	123	51.72	4.80	2.49	25.20	57,863	16,749	246	934	14,592
8/15/63	124	52.53	3.15	1.58	20.79	42,396	16,749	195	774	10,601
	125	52.33	3.38	1.66	20.79	45,309	16,749	223	879	11,278
	126	52.43	3.66	1.64	20.79	48,272	16,749	209	826	12,126
	127	53.83	3.98	1.76	20.79	51,402	16,749	227	896	12,896
	128	22.2	4.20	1.80	20.79	54,849	16,749	215	850	13,867
8/16/63	129	17.0	3.26	1.60	20.79	42,256	4,070	188	745	10,593
	130	18.6	3.55	1.64	20.79	45,169	4,070	187	741	11,378
	131	20.9	3.96	1.76	21.04	48,272	4,070	199	798	12,154
8/20/63	132	16.2	3.11	1.52	19.53	42,256	17,168	212	786	10,552
	133	16.0	3.08	1.48	19.53	42,256	17,168	218	808	10,530
8/29/63	134	0	0.19	0.022	25.2	2,099	17,278	209	996	0
	135	0	0.19	0.054	25.2	2,671	28,720	239	1135	0
	136	0	0.19	0.087	24.7	2,636	28,720	191	895	0
	137	0	0.19	0	24.57	2,636	15,927	188	876	0
	138	0	0.19	0	24.07	2,636	20,875	199	908	0
8/30/63	139	26.8	5.03	2.21	21.8	63,473	17,845	255	1053	15,978
	140	26.4	4.96	2.34	21.8	63,740	29,355	241	997	16,105
	141	26.4	4.96	2.35	21.8	63,473	29,459	243	1005	16,026
9/19/63	142	54.46	4.36	1.74	18.65	59,034	24,502	252	889	14,951
10/8/63	143	52.84	4.16	1.69	18.5	51,096	17,087	244	855	12,855
	144	53.35	3.98	1.56	17.1	53,946	17,087	248	802	13,672
	145	53.77	4.11	1.44	17.0	57,698	17,087	247	794	14,687
	146	53.18	3.80	1.36	17.0	50,066	17,087	238	765	12,668
10/29/63	147	54.89	1.60	0.942	17.39	28,162	38,688	232	762	6,794
	148	54.89	1.58	0.928	17.39	28,162	38,688	227	746	6,810
	149	54.59	1.63	0.928	17.39	28,162	38,688	221	727	6,829
	150	54.48	1.72	0.935	17.39	27,984	38,688	221	727	6,782
	151	55.88	1.90	0.892	17.51	28,938	29,999	272	896	6,869
	152	55.88	1.98	0.899	17.51	28,938	29,999	257	849	6,916
	153	55.68	2.16	0.910	17.51	29,938	29,999	248	819	6,946

(See last page of this figure for footnotes)

FIG 21

EXPEREMENTAL DATA

CONTINUED

Run No.	Preboiler Exit Quality	Preboiler Average Tube to Shell ΔT (F)	Preboiler Over-all Heat Trans. Coefficient (Btu/hr-ft^2 F)	Test Boiler Tube to Shell ΔT(e) (F)	Test Boiler Boiling ΔT(e) (F)	Test Boiler Local Heat Trans. Coeff.(e) (Btu/hr-ft^2 F)	Test Boiler Boiling ΔT(f) (F)	Test Boiler Local Heat Trans. Coeff.(f) (Btu/hr-ft^2 F)	Test Boiler Average Quality	Average Tube-Side Pressure in Test Boiler, psia
81	79.6	25	1088	--	--	--	6.23	8,443	87.6	63.20
82	83.3	26	1292	--	--	--	30.0	1,757	91.2	63.37
83	7.46	8	818.8	--	--	--	2.68	19,142	15.29	61.72
84	0	a	--	--	--	--	2.52	20,556	7.7	62.69
85	0	a	--	--	--	--	0.96	17,448	2.47	60.08
86	0	a	--	--	--	--	1.83	15,301	4.09	58.68
87	0	a	--	--	--	--	1.69	23,550	6.08	59.84
88	0	a	--	--	--	--	1.88	27,394	7.98	60.87
89	89.14	24	2099	37.0	30.6	1,420	c	--	95.59	63.12
90	77.89	20	2154	d	--	--	c	--	82.89	64.22
91	77.61	25	1723	55.0	50.1	663	c	--	82.61	62.19
92	71.0	20	2044	d	--	--	d	--	75.65	64.49
93	94.68	22	2290	d	--	--	d	--	95.32	64.52
94	93.22	24	2279	d	--	--	d	--	93.8	63.62
95	99.91	29	1976	15.0	13.89	501	c	--	100.92	61.51
96	84.76	23	2022	d	--	--	d	--	85.42	66.38
97	66.77	25	1539	1.0	70.28	15,257	c	--	67.4	59.51
98	74.91	22	1958	63.0	60.49	274	c	--	77.35	61.20
99	75.56	23	1843	d	--	--	d	--	77.38	61.22
100	76.72	23	1843	d	--	--	d	--	80.4	62.33
101	78.58	24	1767	6.0	1.23	26,211	c	--	83.63	62.57
102	52.6	21	2208	d	--	--	c	--	55.74	67.61
103	50.33	19	2225	d	--	--	d	--	52.8	68.32
104	50.15	18	2348	d	--	--	d	--	51.87	68.82
105	75.9	25	2027	d	--	--	d	--	77.32	64.11
106	75.9	25	2027	d	--	--	d	--	77.99	64.11
107	76.07	24	2112	d	--	--	d	--	79.09	64.35
108	75.16	22	2303	d	--	--	d	--	79.25	64.77
109	91.98	22	2691	18.0	13.26	2,465	c	--	96.22	65.42
110	50.98	21	2006	d	--	--	d	--	52.74	66.03
111	54.79	19	2373	d	--	--	d	--	56.6	68.71
112	46.72	20	1939	d	--	--	d	--	48.51	66.14
113	41.8	20	1780	d	--	--	d	--	43.56	64.58
114	35.58	21	1543	d	--	--	d	--	40.37	63.11
115	39.92	21	1557	3.0	0.41	41,834	c	--	40.74	60.62
116	39.31	21	1563	d	--	--	c	--	41.11	60.77
117	29.24	22	1185	3.0	0.47	35,636	c	--	30.97	58.67
118	54.78	21	2151	d	--	--	d	--	56.52	65.40
119	59.10	21	2299	d	--	--	d	--	60.86	66.20
120	59.42	21	2299	d	--	--	d	--	61.18	66.98
121	63.55	11	4688	d	--	--	d	--	65.30	68.52
122	67.60	24	2279	3.0	0.47	35,636	c	--	69.34	67.90
123	71.66	25	2315	4.0	1.47	11,394	c	--	73.40	68.76
124	62.80	24	1767	4.0	1.47	11,394	c	--	64.90	62.22
125	66.81	23	1970	d	--	--	d	--	68.91	62.63
126	71.92	24	2011	g	--	--	2.33	7,188	74.02	63.33
127	76.58	25	2056	--	--	--	4.55	3,681	78.68	65.35
128	82.35	25	2194	--	--	--	4.64	3,610	84.45	65.38
129	62.75	22	1921	d	--	--	d	--	63.26	61.48
130	67.40	23	1964	d	--	--	d	--	67.91	62.26
131	71.32	24	2011	d	--	--	d	--	71.82	64.61
132	66.54	24	1761	3.0	0.41	41,873	d	--	68.83	62.75
133	66.40	24	1761	4.0	1.41	12,176	d	--	68.69	61.69
134	0	a	--	g	--	--	5.06	3,409	1.78	58.82
135	0	a	--	g	--	--	6.55	4,385	2.96	58.94
136	0	a	--	g	--	--	6.67	4,306	3.02	59.65
137	0	a	--	--	--	--	3.55	4,486	1.68	59.15
138	0	a	--	--	--	--	3.17	6,585	2.25	58.40
139	90.60	24	2645	g	--	--	5.16	3,458	92.74	65.88
140	91.21	26	2452	8.0	3.64	8,065	5.86	5,009	94.73	64.89
141	90.76	26	2441	g	--	--	6.09	4,837	94.29	65.55
142	98.85	33	1789	36.0	32.35	757.4	33.96	721.50	102.28	63.60
143	85.7	29	1762	g	--	--	1.09	15,676	88.11	63.26
144	98.6	28	1927	7	4.422	3,864	4.77	3,582	101.21	63.17
145	106.5	30	1923	b	--	--	b	--	100+	63.01
146	91.8	39	1284	61	58.42	292.5	c	--	94.42	61.13
147	48.0	23	1224	g	--	--	1.55	24,960	53.79	61.10
148	48.11	23	1224	g	--	--	1.46	26,499	53.90	61.02
149	48.24	23	1224	7	1.29	29,991	1.59	24,332	54.03	60.77
150	47.91	23	1217	g	--	--	1.59	24,332	53.70	60.69
151	48.25	22	1315	g	--	--	1.16	25,861	52.71	61.92
152	48.58	22	1315	g	--	--	1.20	24,999	53.04	61.87
153	48.79	21	1378	g	--	--	1.12	26,785	53.25	61.82

(See last page of this figure for footnotes)

FIG 21

EXPEREMENTAL DATA

CONTINUED

Date	Run No.	Condenser-Discharge Static Pressure (psia)	Preboiler Tube-Side Pressure Drop (psi)	Test Boiler Tube-Side Pressure Drop (psi)	Mass Flow Rate (lb/hr)	Preboiler Boiling Heat Flux (Btu/hr-ft^2)	Test Boiler Boiling Heat Flux (Btu/hr-ft^2)	Preboiler Subcool ΔT, (F)	Preboiler Heat Into Preheat (Btu/hr)	Preboiler Heat Into Boiling (Btu/hr)
10/31/63	154	56.78	1.94	0.773	16.00	30,566	10,051	259	782	7,419
	155	56.58	1.85	0.751	15.88	30,566	10,051	252	755	7,446
	156	56.58	1.76	0.740	15.88	30,566	10,051	241	723	7,478
	157	56.48	1.65	0.740	15.75	30,566	10,041	241	717	7,484
	158	57.04	1.62	0.953	17.14	27,412	48,891	249	806	6,549
	159	57.14	1.60	0.946	17.01	27,412	49,891	254	815	6,540
	160	57.14	1.60	0.946	17.01	27,412	49,891	254	815	6,540
	161	57.14	1.59	0.946	17.01	27,412	49,891	254	815	6,540
	162	56.94	1.56	0.986	17.01	26,598	59,837	249	800	6,337
	163	56.94	1.56	0.986	17.01	26,598	59,837	259	831	6,306
	164	56.94	1.56	0.989	17.01	26,598	59,837	259	831	6,306
	165	56.94	1.56	0.986	17.01	26,598	59,837	259	831	6,306
	166	57.14	2.01	0.935	16.63	26,598	59,837	260	816	6,321
11/1/63	167	57.34	1.81	0.960	17.01	26,598	59,837	271	871	6,266
	168	55.98	2.12	1.040	17.39	25,796	69,985	273	895	6,027
	169	55.68	2.01	1.047	17.39	25,796	69,985	267	877	6,045
	170	54.74	1.67	1.047	17.39	25,796	69,985	262	861	6,061
	171	54.64	1.78	1.047	17.39	25,796	69,985	262	861	6,061
	172	54.54	1.87	1.040	17.39	25,796	69,985	261	857	6,065
	173	54.54	1.87	1.032	17.26	25,796	69,985	261	851	6,078
	174	1415	1.89	2.152	16.38	51,249	20,198	184	567	13,194
	175	1430	2.00	2.058	15.75	51,249	18,087	183	542	13,209
	176	1445	1.87	2.014	15.50	51,264	18,264	175	511	13,240
11/2/63	177	39.84	4.20	2.0	17.25	50,000	16,900	182	591	12,829
	178	39.5	4.99	1.82	17.0	49,900	16,900	181	584	12,786
	179	40.78	4.65	1.78	17.0	49,900	16,900	182	586	12,784
	180	40.78	5.06	1.81	17.0	49,900	16,900	185	596	12,774
11/3/63	181	39.69	4.99	1.87	17.4	49,800	7,770	179	591	12,759
	182	39.35	4.70	1.795	16.6	49,900	7,770	158	499	12,881
11/4/63	183	39.77	4.67	1.805	17.3	55,294	7,955	188	617	14,219
	184	40.5	4.90	1.834	17.6	55,459	8,181	177	591	14,290
11/5/63	185	42.2	5.1	1.829	17.6	50,944	9,245	169	565	13,104
	186	42.2	5.14	1.823	17.6	50,944	9,245	169	565	13,104
	187	42.79	5.5	1.955	18.6	54,378	10,962	192	678	13,912
	188	39.78	5.69	2.2	19.5	54,543	17,087	174	645	13,990
	189	39.78	5.8	2.2	19.5	54,543	17,087	175	649	13,986
11/9/63	190	35.02	5.21	1.92	16.9	50,371	17,337	197	629	12,886
	191	35.02	5.14	1.93	16.9	50,391	17,337	197	629	12,886
	192	37.23	5.06	1.96	17.6	50,371	17,337	197	656	12,859
	193	36.93	5.08	1.98	17.6	50,371	17,337	196	652	12,863
	194	36.83	5.01	1.95	17.5	54,543	13,331	200	661	13,974
11/10/63	195	36.76	4.56	1.75	16.0	47,064	17,337	165	500	12,128
	196	36.86	4.52	1.75	16.0	47,064	17,337	165	500	12,128
	197	33.04	4.94	1.95	16.4	42,256	17,337	164	509	10,829
11/11/63	198	35.27	5.14	1.99	17.3	46,568	17,337	196	640	11,855
	199	35.16	5.24	2.01	17.5	46,568	17,337	201	664	11,831
11/17/63	200	36.29	1.11	0.81	17.01	21,039	17,676	142	457	5,188
11/20/63	201	41.0	4.05	7.29	18.52	43,731	17,087	142	498	11,236
	202	40.38	4.00	7.08	18.52	43,731	17,087	142	498	11,236
	203	40.25	3.98	7.04	18.52	43,731	17,087	144	505	11,229
	204	40.0	3.94	6.80	18.52	43,731	17,087	148	519	11,215
11/21/63	205	36.59	4.74	1.84	16.76	41,594	17,514	176	559	10,601
11/22/63	206	38.57	6.69	1.88	17.26	55,459	17,514	211	688	14,193
	207	37.67	3.51	1.62	17.26	42,396	17,514	184	601	10,774
	208	37.97	3.51	1.61	17.26	42,396	17,514	185	604	10,771
	209	37.27	3.66	1.65	17.26	42,396	17,514	185	604	10,771
	210	37.17	3.98	1.63	17.26	42,256	17,514	185	604	10,734
	211	35.06	4.97	1.81	17.64	46,924	17,514	181	605	11,985
	212	34.96	5.01	1.81	17.64	46,924	17,684	180	601	11,989
11/24/63	213	36.66	3.22	1.55	17.14	39,368	17,514	174	564	9,999
	214	36.46	3.17	1.56	17.14	39,368	17,514	173	561	10,002
11/28/63	215	52.82	2.12	*	20.16	31,177	*	314	1183.8	7,181
	216	53.82	2.90	*	16.63	41,836	*	284	887.9	10,337
	217	53.80	3.08	*	16.76	45,493	*	286	901.2	11,305
	218	53.10	3.33	*	16.38	49,913	*	287	883.8	12,508
	219	52.19	3.31	*	16.51	49,761	*	278	863.3	12,489
11/29/63	220	52.34	2.90	*	16.38	41,836	*	248	766.1	10,459
	221	52.29	3.11	*	16.38	45,639	*	252	778.5	11,468
	222	52.35	3.31	*	16.13	49,913	*	254	772.7	12,619
	223	51.95	3.10	*	16.00	49,346	*	256	771.7	12,468
11/30/63	224	51.45	3.71	*	17.51	54,219	*	269	887.4	13,661
	225	51.43	3.87	*	17.39	54,596	*	260	852.7	13,796
	226	50.99	3.53	*	16.51	49,455	*	250	778.5	12,492
12/1/63	227	52.11	3.29	*	16.38	49,608	*	256	790.4	12,521
	228	52.51	3.51	*	17.64	49,913	*	254	845.9	12,546
	229	52.26	3.33	*	17.01	49,043	*	265	849.2	12,310
12/2/63	230	51.23	3.37	*	16.63	49,332	*	254	796.7	12,440
12/3/63	231	24.94	5.45	*	17.01	49,760	*	285	902	12,450
12/4/63	232	25.73	6.65	*	17.39	54,973	*	352	1133	13,617
	233	25.63	6.33	*	17.39	54,596	*	351	1129.2	13,520
	234	51.78	3.38	*	17.01	49,608	*	258	827.7	12,483
12/5/63	235	51.60	3.38	*	17.64	49,913	*	249	829.3	12,563

(See last page of this figure for footnotes)

FIG 21

EXPEREMENTAL DATA

CONTINUED

Run No.	Preboiler Exit Quality	Preboiler Average Tube to Shell ΔT (F)	Preboiler Over-all Heat Trans. Coefficient (Btu/hr-ft^2 F)	Test Boiler Tube to Shell ΔT(e) (F)	Test Boiler Boiling ΔT(e) (F)	Test Boiler Local Heat Trans. Coeff.(e) (Btu/hr-ft^2 F)	Test Boiler Boiling ΔT(f) (F)	Test Boiler Local Heat Trans. Coeff.(f) (Btu/hr-ft^2 F)	Test Boiler Average Quality	Average Tube-Side Pressure in Test Boiler, psia
154	57.03	18	1698	--	--	--	1.50	6, 701	58.67	62.35
155	57.68	19	1609	--	--	--	1.41	7, 128	59.33	62.06
156	57.92	17	1798	--	--	--	1.38	7, 283	59.57	61.96
157	58.45	17	1798	--	--	--	1.38	7, 283	60.11	61.85
158	47.05	16	1713	--	--	--	0.45	110, 869	54.64	63.66
159	47.35	15	1827	--	--	--	0.45	110, 869	55.00	63.71
160	47.35	15	1827	--	--	--	0.41	121, 685	55.00	63.72
161	47.35	15	1827	--	--	--	0.67	74, 464	55.00	63.71
162	45.88	15	1773	--	--	--	0.65	92, 057	55.05	63.74
163	45.66	15	1773	--	--	--	0.79	75, 743	54.83	63.75
164	45.66	15	1773	--	--	--	0.83	72, 093	54.83	63.77
165	45.66	15	1773	--	--	--	0.83	72, 093	54.83	63.77
166	46.81	13	2046	--	--	--	0.74	80, 861	56.19	63.57
167	45.37	14	1900	--	--	--	2.22	26, 954	54.54	64.08
168	42.68	17	1517	--	--	--	3.22	21, 080	53.18	63.08
169	42.81	16	1612	--	--	--	3.14	22, 288	53.31	62.71
170	42.87	15	1720	--	--	--	2.05	34, 139	53.35	61.85
171	42.87	14	1843	--	--	--	2.01	34, 818	53.35	61.76
172	42.90	15	1720	--	--	--	2.05	34, 139	53.38	61.63
173	43.27	15	1720	--	--	--	2.01	34, 818	53.83	61.62
174	97.80	58	883.6	169	165.97	121.70	c	--	100.97	43.03
175	101.91	54	949.1	b	--	--	c	--	100+	42.84
176	103.66	59	868.6	b	--	--	c	--	100+	42.54
177	91.2	87	574.7	99	96.45	175.5	c	--	93.75	52.42
178	92.2	88	567.0	103	100.45	168.5	c	--	94.79	51.40
179	92.1	84	594.0	102	99.45	170	c	--	94.69	52.15
180	92.0	71	702.8	100	97.45	173.5	c	--	94.59	52.19
181	89.8	72	691.7	69	67.77	115	c	--	90.96	52.04
182	95.0	86	580.2	78	76.77	101.5	c	--	96.22	51.06
183	100.7	67	825.3	82	80.75	98.5	c	--	101.90	52.24
184	99.5	81	684.7	65	63.71	128.4	c	--	100.71	51.69
185	91.2	80	636.8	81	79.56	116.2	c	--	92.56	53.11
186	91.2	71	717.5	88	86.56	106.8	c	--	92.56	53.09
187	91.8	61	891.4	78	76.31	143.7	c	--	93.33	55.40
188	87.9	67	814.1	106	103.42	165.2	c	--	90.18	53.37
189	87.9	61	894.1	111	108.42	157.6	c	--	90.18	53.42
190	93.2	62	812.4	100	97.39	178.0	c	--	95.85	48.20
191	93.2	55	915.8	111	108.39	160.0	c	--	95.85	48.30
192	89.4	59	853.7	103	100.39	172.7	c	--	91.95	50.40
193	89.5	51	987.7	111	108.39	160.0	c	--	92.05	50.26
194	97.7	47	1160	117	114.97	116.0	c	--	99.68	50.16
195	92.55	53	880	78	75.39	230.0	c	--	95.35	47.60
196	92.55	49	960.5	88	85.39	203.0	c	--	95.35	47.65
197	80.52	46	918.6	99	96.39	179.9	c	--	83.25	45.92
198	83.67	51	913.1	54	51.39	337.4	c	--	86.26	48.15
199	82.65	46	1012.3	g	--	--	12.87	1, 347	85.22	48.94
200	37.06	72	292.2	4	1.34	13, 191	c	--	39.74	45.99
201	73.81	65	672.8	d	--	--	d	--	76.19	52.38
202	73.81	66	662.6	d	--	--	d	--	76.19	51.82
203	73.76	65	672.8	d	--	--	d	--	76.14	51.69
204	73.67	65	672.8	d	--	--	d	--	76.05	51.43
205	77.23	53	784.8	63	60.36	290.2	28.40	616.7	79.93	48.57
206	100+	30	1848.6	b	--	--	c	--	100+	50.79
207	76.22	21	2018.9	d	--	--	d	--	78.85	49.56
208	76.20	21	2018.9	d	--	--	d	--	78.83	49.74
209	76.20	21	2018.9	d	--	--	d	--	78.83	49.45
210	75.93	21	2012.2	d	--	--	d	--	78.56	49.30
211	83.06	17	2760.2	--	--	--	0.39	44, 908	85.63	49.29
212	83.08	18	2606.9	--	--	--	0.37	47, 795	85.68	49.21
213	71.14	20	1968.4	d	--	--	d	--	80.29	47.75
214	71.16	22	1789.5	d	--	--	d	--	80.31	47.67
215	43.76	17	1834	*	*	*	*	*	*	*
216	76.55	22	1902	*	*	*	*	*	*	*
217	83.07	24	1896	*	*	*	*	*	*	*
218	94.04	26	1920	*	*	*	*	*	*	*
219	93.04	27	1843	*	*	*	*	*	*	*
220	78.54	27	1549	*	*	*	*	*	*	*
221	86.12	27	1690	*	*	*	*	*	*	*
222	96.23	33	1513	*	*	*	*	*	*	*
223	95.73	41	1204	*	*	*	*	*	*	*
224	96.08	33	1643	*	*	*	*	*	*	*
225	97.70	32	1706	*	*	*	*	*	*	*
226	93.06	31	1595	*	*	*	*	*	*	*
227	94.02	31	1600	*	*	*	*	*	*	*
228	87.59	25	1997	*	*	*	*	*	*	*
229	89.02	28	1752	*	*	*	*	*	*	*
230	92.01	26	1897	*	*	*	*	*	*	*
231	89.15	51	975.7	*	*	*	*	*	*	*
232	95.49	79	695.9	*	*	*	*	*	*	*
233	94.70	59	925.4	*	*	*	*	*	*	*
234	90.38	26	1908	*	*	*	*	*	*	*
235	87.71	27	1849	*	*	*	*	*	*	*

*Boiler No. 2 isolated from the system

a - Single phase flow in preboiler - exit quality <5%

b - Superheat - quality >100%

c - Tube to shell pressure differential indicated over scale. Calculations based on absolute pressure readings.

d - Tube to shell pressure differential gage (PI-21) not operating during these runs - NaK line frozen. Temperature differential (tube to shell) was not sufficient (<5F) to permit usage of the absolute pressures.

e - From absolute pressure measurement

f - From differential pressure measurement

g - Differential pressure gage was used because of small pressure differences

FIG 22

FORCED CONVECTION LOCAL BOILING HEAT TRANSFER COEFFICIENTS

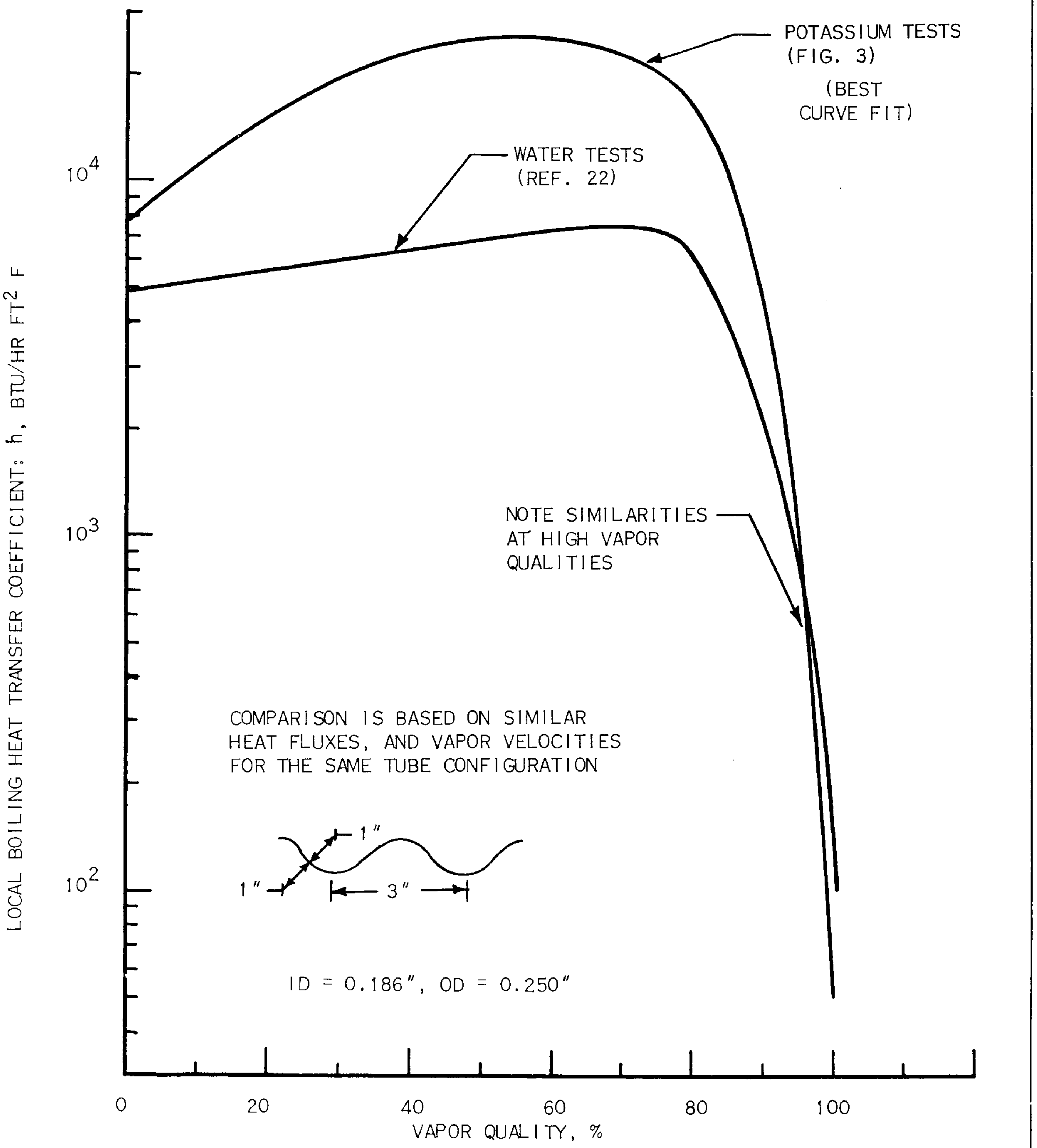

FIG 23

BAND OF EXPERIMENTAL ERROR

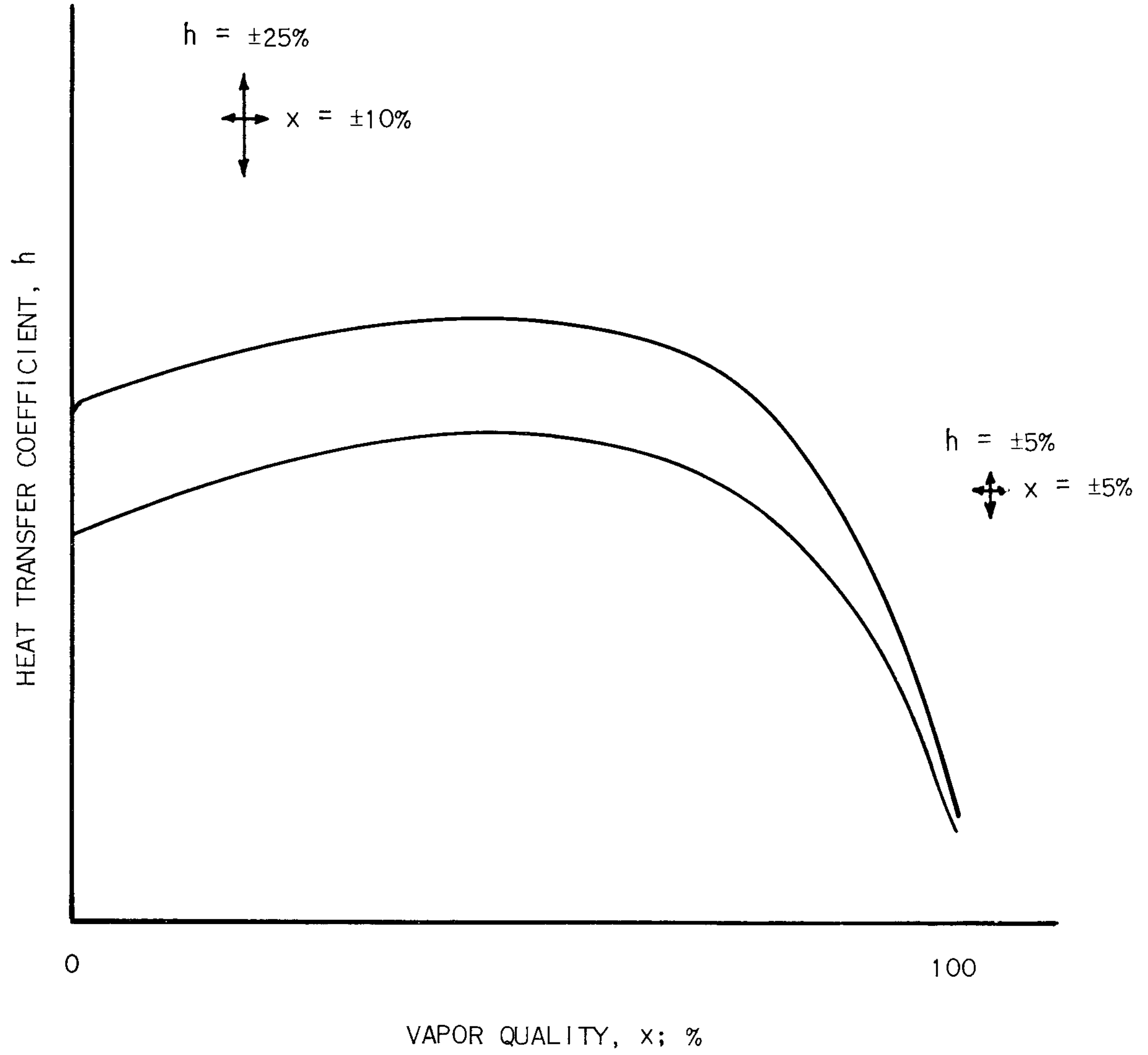

OVER-ALL HEAT TRANSFER COEFFICIENT, U, FOR THE POTASSIUM PREBOILER IN THE P&WA BOILING POTASSIUM HEAT TRANSFER TEST

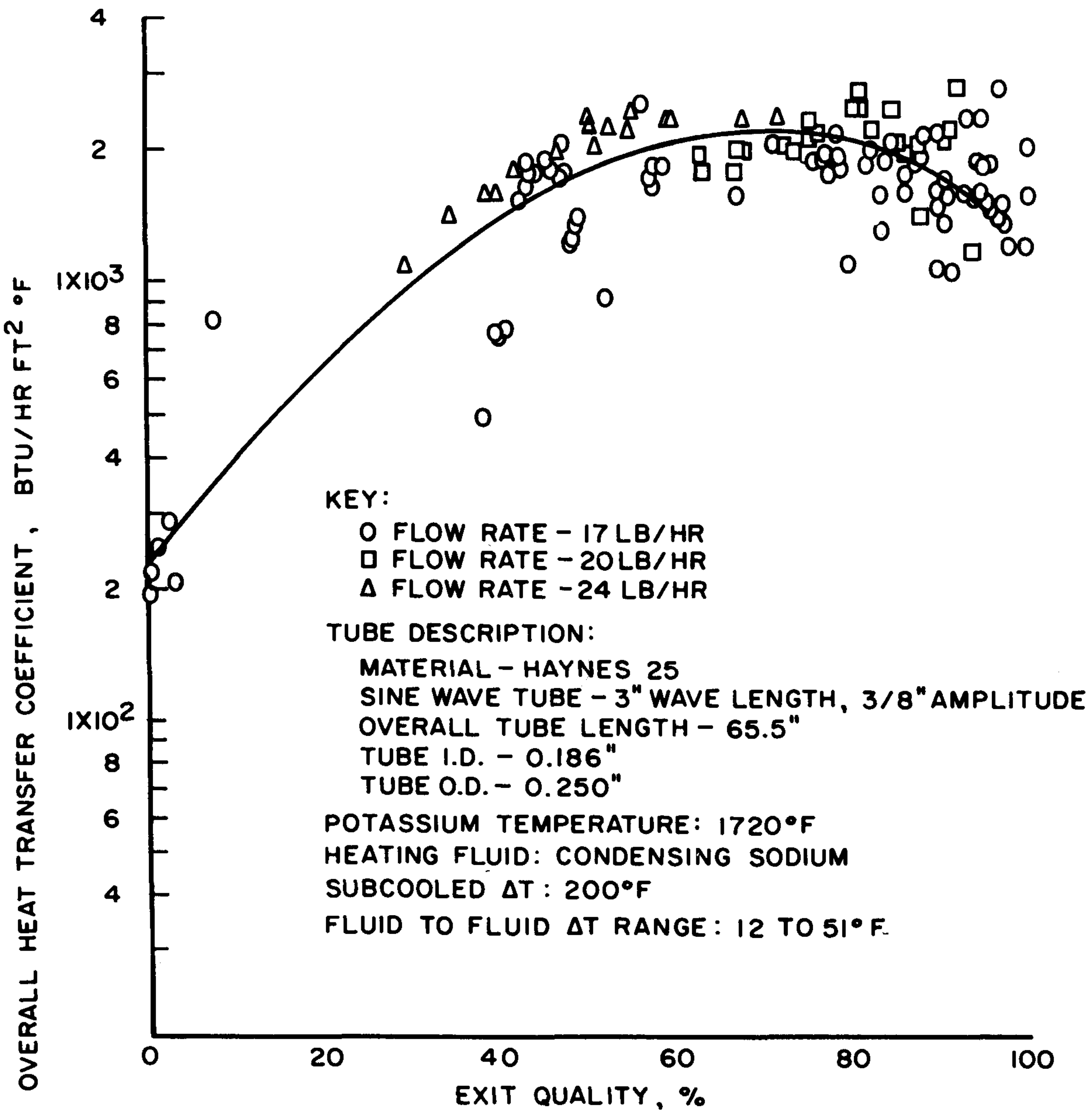

KEY:

- O FLOW RATE - 17 LB/HR
- □ FLOW RATE - 20 LB/HR
- Δ FLOW RATE - 24 LB/HR

TUBE DESCRIPTION:

- MATERIAL - HAYNES 25
- SINE WAVE TUBE - 3" WAVE LENGTH, 3/8" AMPLITUDE
- OVERALL TUBE LENGTH - 65.5"
- TUBE I.D. - 0.186"
- TUBE O.D. - 0.250"

POTASSIUM TEMPERATURE: 1720°F

HEATING FLUID: CONDENSING SODIUM

SUBCOOLED ΔT: 200°F

FLUID TO FLUID ΔT RANGE: 12 TO 51° F

FIG 24

C. Two-Phase Stability Experience

1. Preheater

The achievement of loop stability was a continuing problem despite the high pressure drop in the liquid portion of the loop. Much of the instability appeared to originate in the preheater as a result of subcooled nucleate boiling. This boiling phenomenon is a result of a temperature gradient in the boundary layer which can result in local temperature higher than saturation. A bubble is formed at the wall, swept into the core or cooler portion of the stream, and consequently collapsed.

This phenomenon was indicated by a preheater surface thermocouple which cycled 50 to 100F. The average wall temperature was about 100F above saturation while the fluid temperature at the exit of the preheater was below saturation. Post-test examination of the preheater also indicated heavier than average oxidation rate. The flow momentarily increased, then decreased below normal and oscillated rapidly when the measured temperature dropped suddenly from a maximum. The preheater inlet pressure oscillated. In time, the flow rate went back to normal, the pressure oscillation stopped, and the preheater surface temperature started to rise again. The cycle repeated itself. This phenomenon was indicative of a bubble being formed at the wall, resulting in liquid being momentarily displaced by the bubble and causing a sudden rise in the indicated flow rate. The bubble or bubbles being formed then caused a general lowering of flow rate by restricting the flow area. The bubble collapsed suddenly when it was swept into the cold portion of the stream, causing additional pressure and flow fluctuations. The cyclic nature of the process stemmed from the thermal inertia of the tube, and the superheat required to initiate boiling.

This form of instability was reduced to a minimum by operating the preheater at the lower heat flux. The preheater outlet temperature could not be reduced without limit, however, as similar pressure and flow oscillations were observed at low preheater outlet temperatures. This indicates subcooled nucleate boiling within the preboiler. Stable operation was observed when the preheater outlet temperature was about 200F below the saturation temperature.

2. Preboiler

A unique form of instability was observed in the preboiler. The boiler would stop boiling periodically, as evidenced by a decrease in the boiling pressure drop and a rise in the shell side pressure. The interface was pictured to move down to the preboiler outlet. This phenomenon could be predicted by observing the preheater inlet pressure. The boiling pressure drop would decrease shortly after this pressure started to oscillate. Boiling was restored by allowing the driving Δt to increase (i.e., increase in shell side temperature). When the shell side pressure reached the maximum allowable pressure and the boiler still would not function, power was cut off and the pressure allowed to drop. In time, the boiler would start to boil again, the heat being supplied from the thermal inertia of the boiler. Power was gradually increased when the preboiler started to function normally. This could also be predicted by a decrease in preheater inlet pressure oscillations.

It is believed that system pressure disturbances had the effect of increasing the temperature required to boil the potassium due to boiling initiation (superheat) requirements. As a consequence of the pressure oscillation, vapor generation increased in the first boiler diminished shell temperature, the boiler pressure drop decreased, and the flow increased. The increase in flow rate reduced the amount of subcooled nucleate boiling. When the pressure oscillation ceased, the preboiler began to operate effectively, and boiling began. A graphical description of this preboiler instability is shown in Fig. 25. Typical oscillations are shown in Figs. 26 and 27.

3. Condenser

The condensing interface could be clearly observed. A uniform tube temperature in the vapor region was followed by a sudden temperature gradient to about 850F. This is shown in Fig. 1. Intermittently, this apparent interface moved a foot downstream. When the interface reached the end of its travel, the temperature level of the entire visible region would drop uniformly by approximately 200F. System pressures and flow would oscillate. In time, the interface would reappear from the upstream section of the condenser and gradually move to its original position. This random cycle took 45 seconds to one minute. Flow stratification with bridging of

EXPLANATION OF PREBOILER INSTABILITY

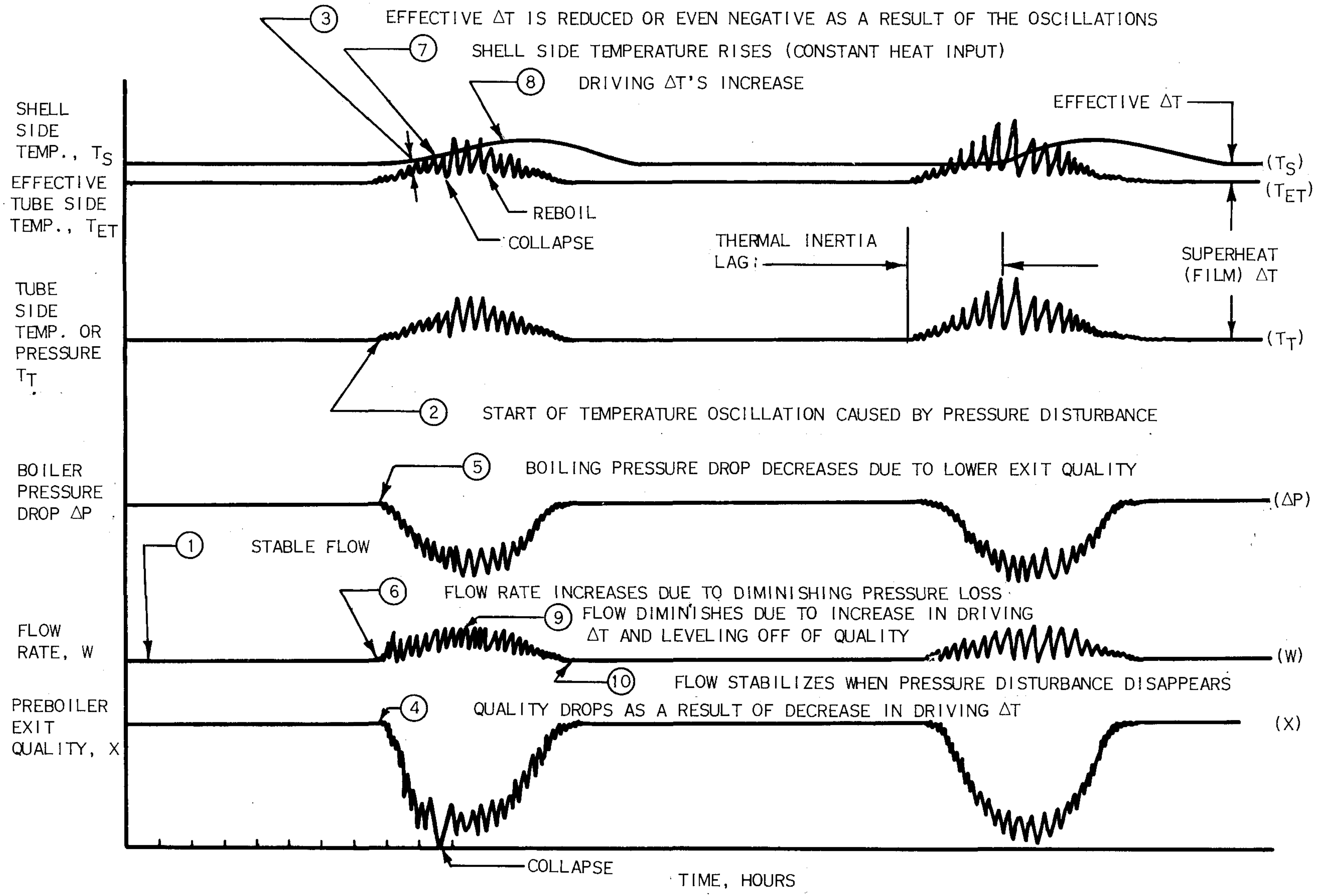

(BUBBLE COLLAPSE AND REBOIL IS NOT A NECESSARY CONDITION FOR CONTINUED PERIODIC OSCILLATION)

FIG 25

FIG 26

TYPICAL STABLE FLOW RATE OSCILLOGRAPH RECORD

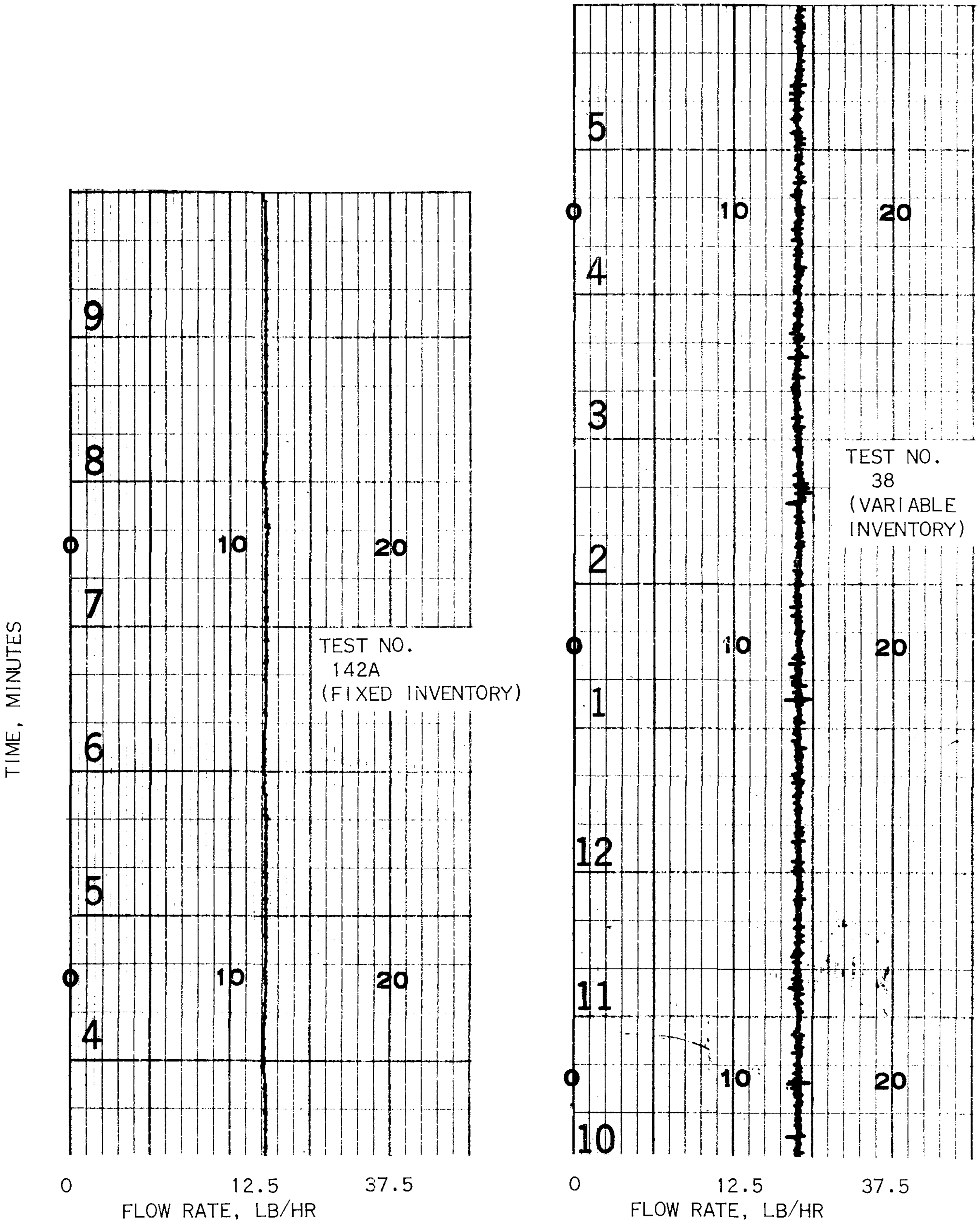

FIG 27

TYPICAL OSCILLOGRAPH RECORD OF FLOW INSTABILITIES

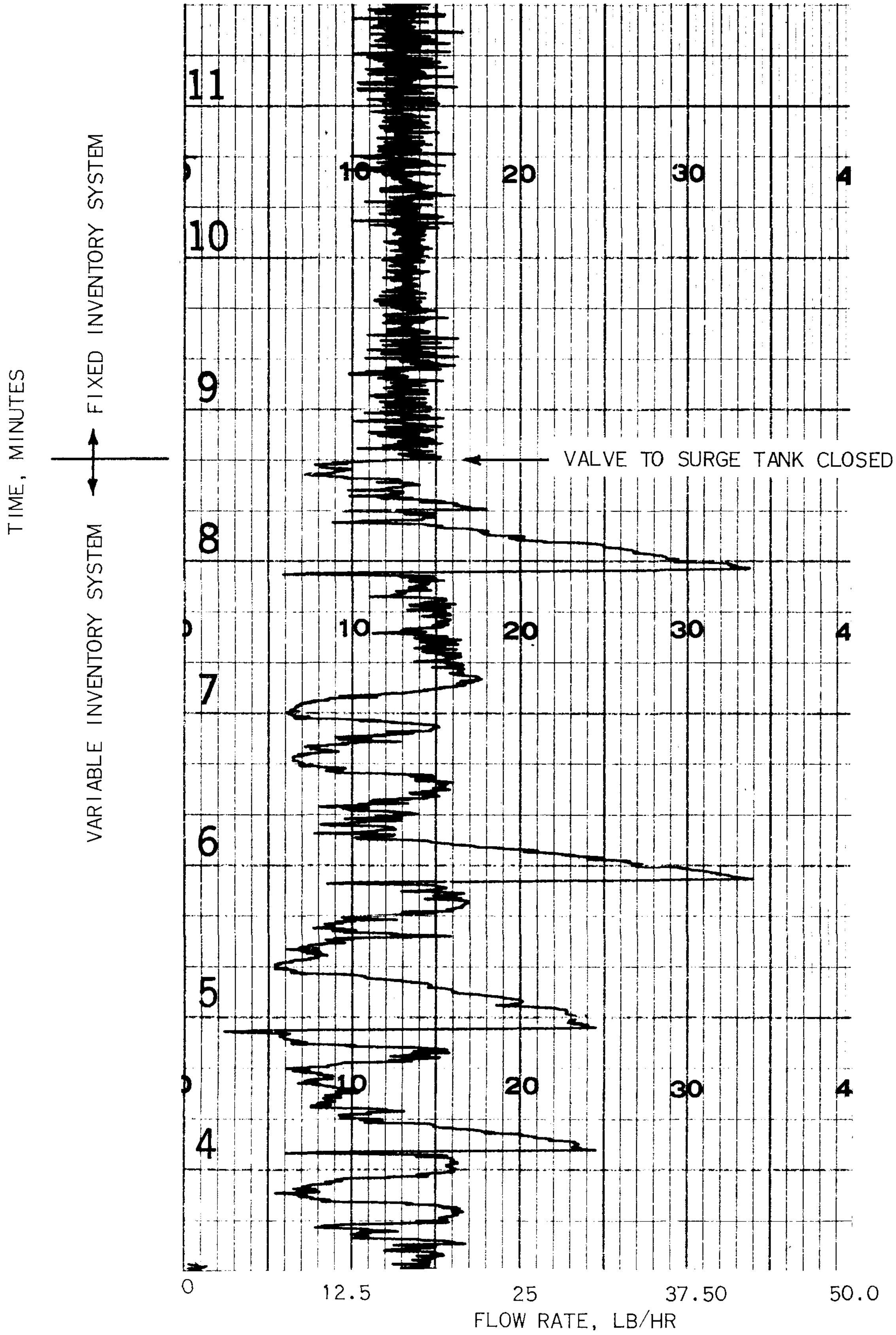

the liquid stream is offered as a possible explanation, since the condenser was sloped two degrees upward. This instability was observed in both hard and soft systems.

4. Miscellaneous System Stability Tests

Several tests were conducted to obtain better insight into the design and operation of two-phase systems. These tests are described below.

a. Effect of liquid pressure drop at the preheater inlet at constant flow, pressure, and degree of subcooling:

Stability improved as the pressure drop was varied from a negligible value to 60 psi. Above 10 psi, however, no significant improvement was observed. At very little pressure drop, the system was highly unstable. Ten psi was comparable to the boiling pressure drop.

b. Effect of pressure drop at the condenser exit:

A valve downstream of the condenser and near the EM flowmeter was throttled to improve stability. A small pressure drop(3 to 5 psi, which corresponded roughly to the condenser pressure drop) resulted in a marked improvement. Above 10 psi, no apparent improvement was observed.

c. Effect of non-condensibles:

Non-condensibles in the potassium circuit seemed to have a definite effect on the loop stability.

At one point in the operation, about 100 hours of continuous boiling time were accumulated with only short periods of stable operation. It was decided to pump the potassium through the calibration tanks to eliminate non-condensibles which were assumed to originate from the helium cover gas during normal operation. After one hour of this mode of operation, stability was obtained.

d. Effect of subcooling:

The amount of subcooling was varied from 100 to 300F at constant flow and pressure.

About 200F subcooling seemed to produce the best compromise. Below this, subcooled nucleate boiling was apparent in the preheater. Above this, subcooled nucleate boiling in the boiler inlet caused instability.

e. Effect of pressure level:

The boiling pressure was varied from 42 psia to 62 psia at constant flow and subcooling.

Stability was improved at the higher boiling pressures, but due to the small pressure range covered, no quantitative statements can be made.

f. Effect of system hardness:

The system was operated with a variable loop inventory (soft) and with a fixed inventory (hard) by valving an expansion tank in or out of the system.

The hard system was more stable; however, the system was more difficult to control since:

1) No bellows-type accumulator was incorporated into the system. Therefore, the loop inventory could not be varied except by opening a valve which required that the pressure in the expansion tank be preset at the proper level for the inventory required.

2) The heat rejection system utilized natural convection. Any drift in the net enthalpy of the system resulted in a drift of the loop pressure. Lack of fine control of the cooling air flow rate resulted in no improvement when forced convection cooling was used instead of natural convection cooling.

The hard system did not prevent the preboiler instability described in Section VI-C-2. Flow recordings made during stable and unstable operation of both soft and hard systems are shown in Figs. 26 and 27, respectively.

g. Effect of condensing length:

The location of the condensing interface was varied. Forced air convection, natural convection, and insulation were all applied to change the location of the interface. No change in the loop stability was noted.

h. Effect of accumulator location:

An alternate accumulator was connected at the preheater inlet to investigate the effect on stability when loop pressure was controlled at this location rather than at the pump inlet.

This mode of operation was quickly discarded. Loop stability was not achieved, and preheater failure by overheating was a real possibility in the event of a prolonged reversal or stoppage of flow.

VII. CHEMISTRY AND METALLURGY

A. Gas System

Helium was chosen as the cover gas, as it is easily purified by cryogenic means. The small quantities of gas needed involved no great expense. The helium was purified (i.e., O_2 and H_2O were removed) by passing it through activated charcoal filters at liquid air temperatures. This method of purification reduced the oxygen content from about 10 ppm in Grade A helium to less than 1 ppm. The water content was reduced from 20 ppm to less than 1 ppm. The all-welded gas system is shown in Fig. 14.

B. Loop Bake-Out

Absorbed gases were removed by heating all liquid metal bearing components to 350F to 400F. Prior to bake-out, the loop was purged with purified helium and evacuated. The loop was then back-filled with helium, and bake-out was started. Water and oxygen content of helium bled from the system were measured. Two parts per million each of O_2 and H_2O was considered satisfactory. A Beckman Moisture Analyzer was used to measure water content and a Lockwood McLorie Oxygen Analyzer was used to measure oxygen content. The decrease in O_2 and H_2O content with time is shown in Figs. 28, 29, 30, and 31 for the loop and all boilers.

C. Liquid Metal History

1. Potassium

The potassium used in this test was purchased from Mine Safety Appliances Co. Sodium-free potassium was specified. The incoming potassium was analyzed, purified, analyzed again, charged into the loop fill and drain tanks, and purified once again. The purification cycle consisted of hot trapping at 1400F for 24 hours with titanium sponge. The purified potassium was vacuum charged at 400F into the system through a 5-micron sintered metal filter. Once charged, the system was heated to 1000F and potassium circulated for two hours, then dumped hot. The potassium was repurified and refiltered before refilling the loop for test operation. The potassium analysis prior to charging the loop is tabulated in Fig. 32.

2. Sodium

The sodium used in this test was purchased from duPont. The purity analysis prior to final filtering indicated 10-31 ppm O_2. The liquid was charged into the loop through a 5 micron filter at 400F.

D. Test Termination

In the interest of obtaining the maximum amount of two-phase operating experience and experimental data, it was decided to continue operation beyond the system design life of 1000 hours.

After approximately 3170 hours at operating temperatures (1800F), including 825 boiling hours, a liquid metal leak occurred at the test boiler drain line junction. This was evidenced by a drop in shell cavity pressure, and by liquid metal smoke. In order to continue obtaining data on the preboiler and superheat boiler, it was decided to isolate the test boiler from the remainder of the system. The failure region was manually cleaned and decontaminated to remove metallic oxides and residual liquid metal. The test boiler drain line was then capped and the shell cavity maintained under an inert gas blanket for the remainder of the test program.

POTASSIUM LOOP GAS PURITY DATA

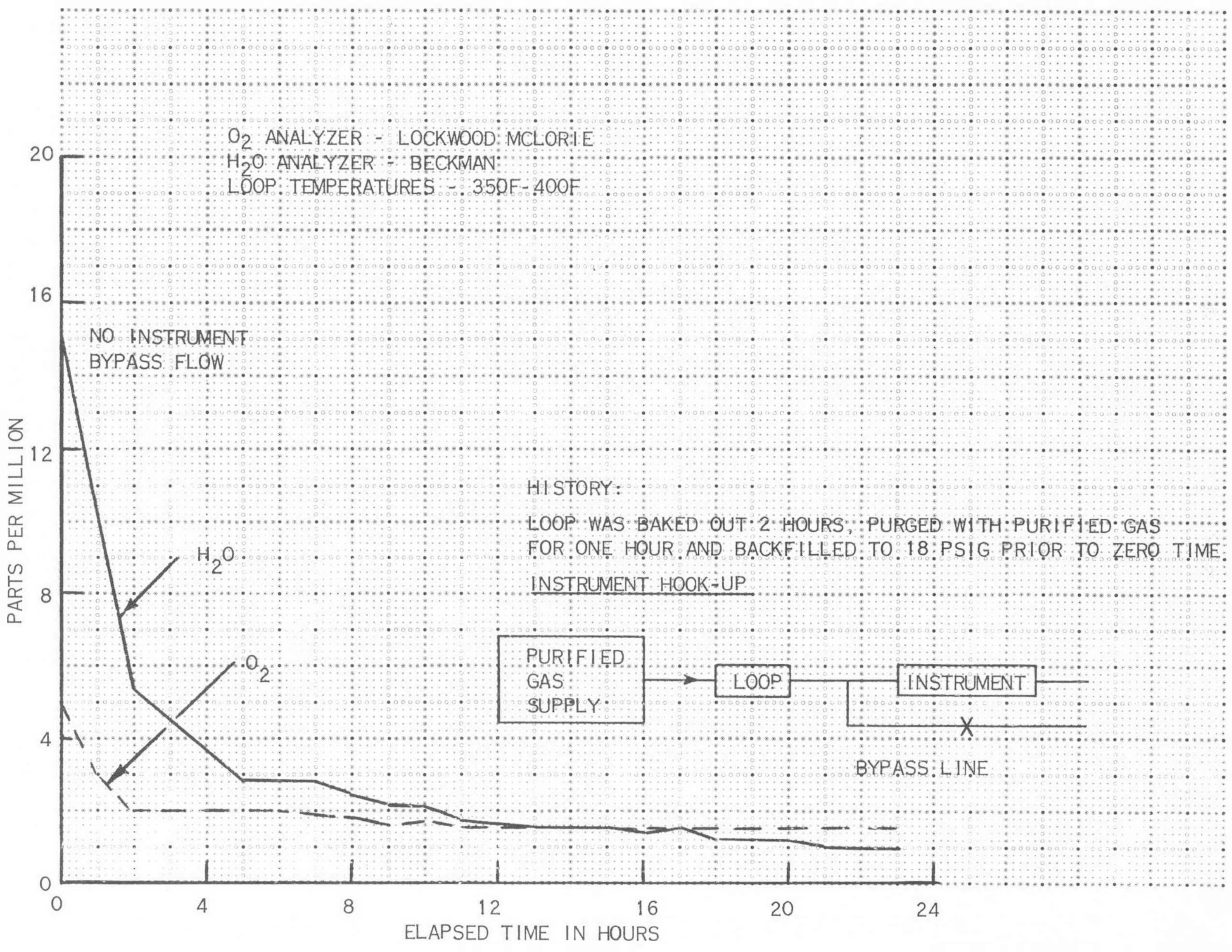

O_2 ANALYZER - LOCKWOOD MCLORIE
H_2O ANALYZER - BECKMAN
LOOP TEMPERATURES - 350F-400F

HISTORY:

LOOP WAS BAKED OUT 2 HOURS, PURGED WITH PURIFIED GAS FOR ONE HOUR AND BACKFILLED TO 18 PSIG PRIOR TO ZERO TIME

FIG 28

PREBOILER EFFLUENT GAS PURITY MEASUREMENT

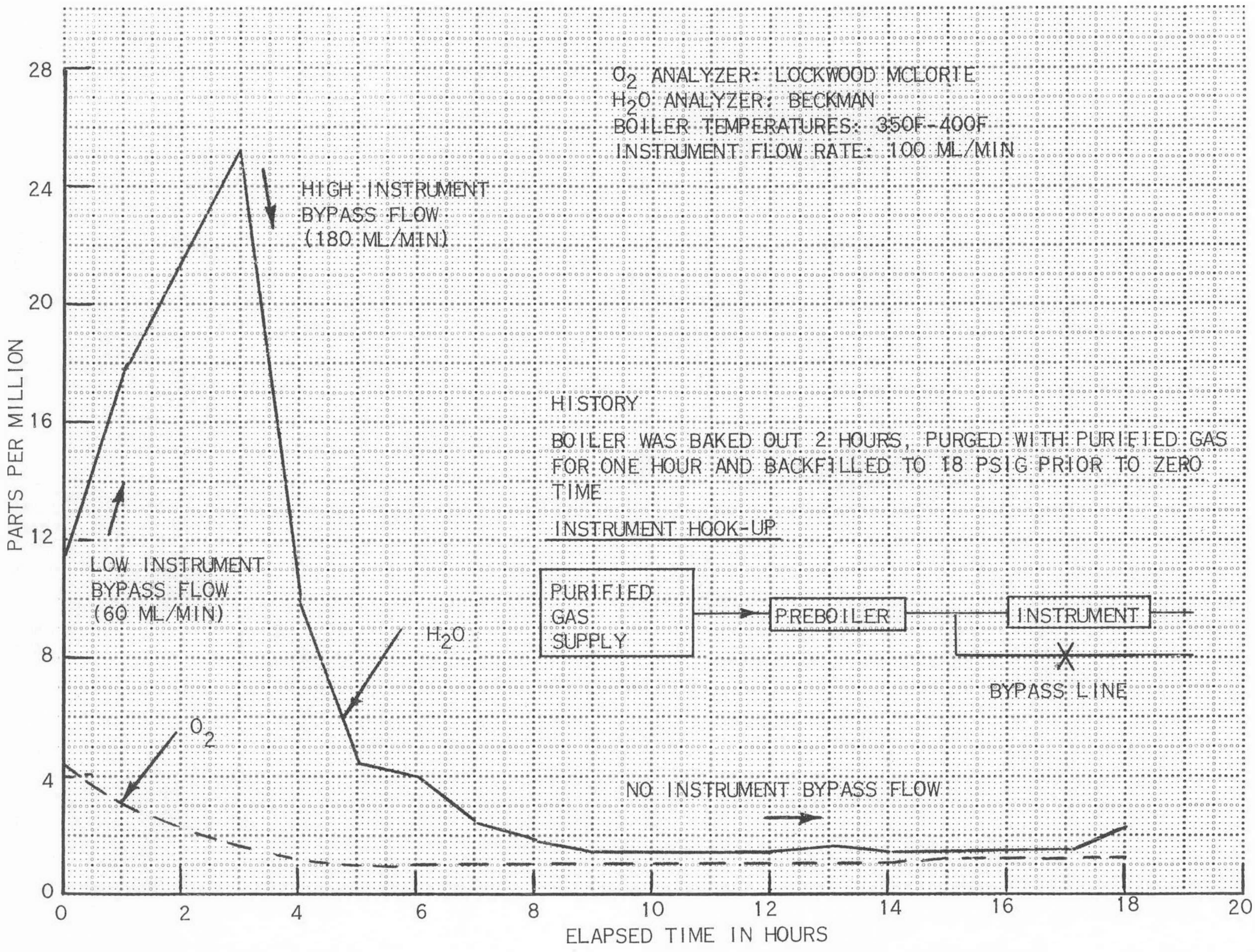

O_2 ANALYZER: LOCKWOOD MCLORIE
H_2O ANALYZER: BECKMAN
BOILER TEMPERATURES: 350F-400F
INSTRUMENT FLOW RATE: 100 ML/MIN

HISTORY

BOILER WAS BAKED OUT 2 HOURS, PURGED WITH PURIFIED GAS FOR ONE HOUR AND BACKFILLED TO 18 PSIG PRIOR TO ZERO TIME

INSTRUMENT HOOK-UP

PWAC - 429
FIG 29

TEST BOILER GAS PURITY MEASUREMENT

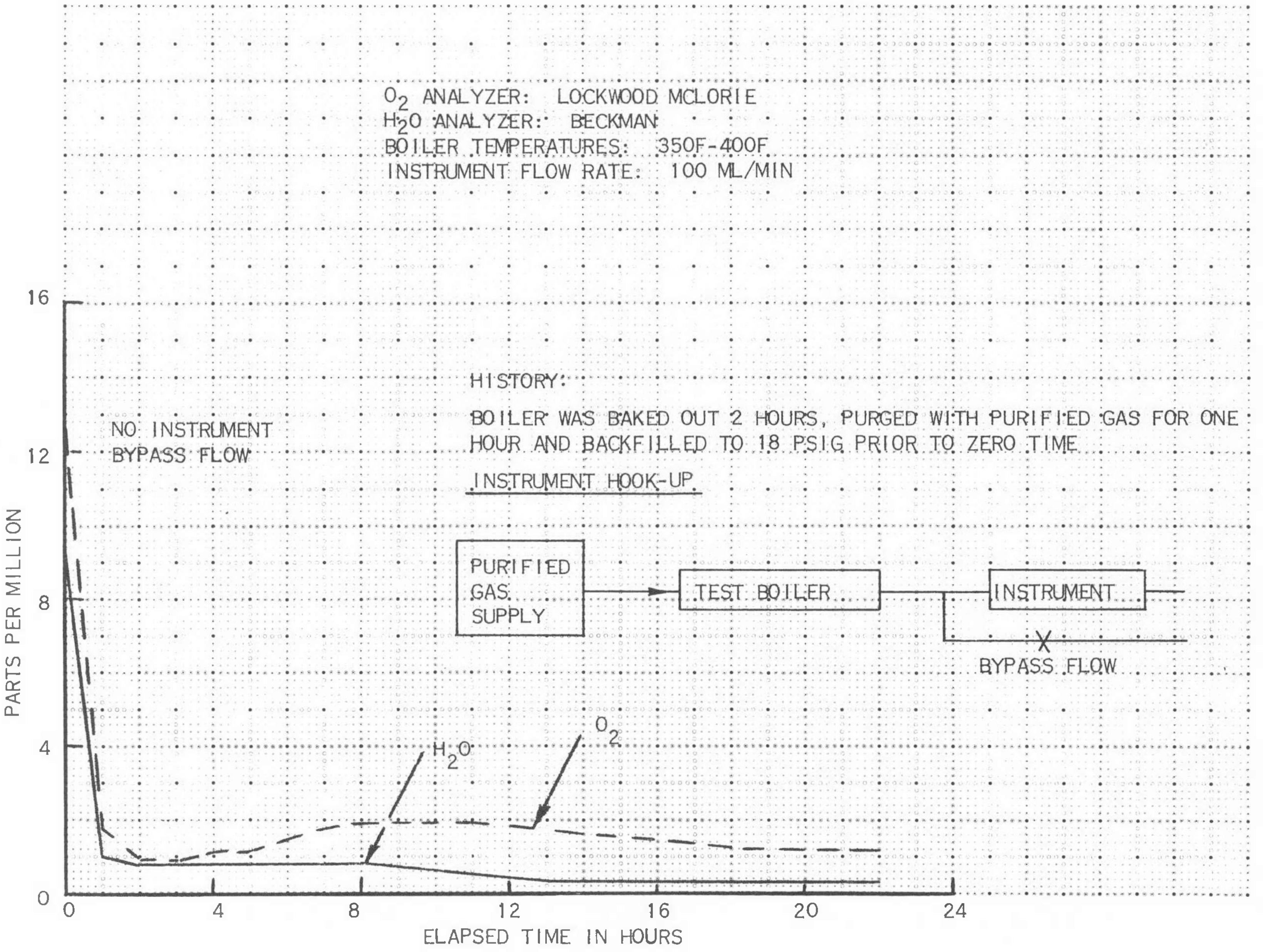

O_2 ANALYZER: LOCKWOOD MCLORIE
H_2O ANALYZER: BECKMAN
BOILER TEMPERATURES: 350F-400F
INSTRUMENT FLOW RATE: 100 ML/MIN

HISTORY:

BOILER WAS BAKED OUT 2 HOURS, PURGED WITH PURIFIED GAS FOR ONE HOUR AND BACKFILLED TO 18 PSIG PRIOR TO ZERO TIME

INSTRUMENT HOOK-UP

FIG 30

SUPERHEATING BOILER EFFLUENT GAS PURITY MEASUREMENT

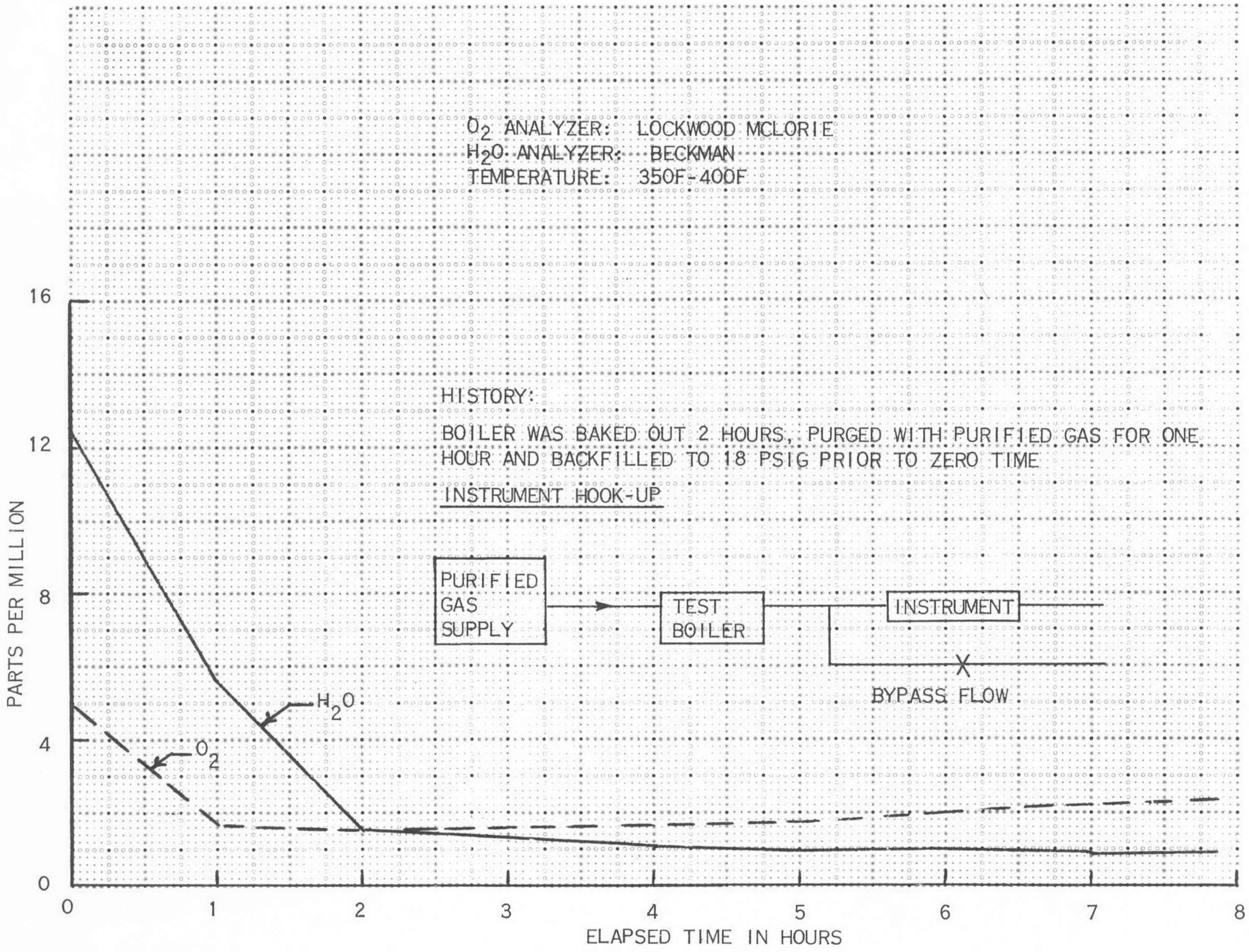

O_2 ANALYZER: LOCKWOOD MCLORIE
H_2O ANALYZER: BECKMAN
TEMPERATURE: 350F-400F

HISTORY:

BOILER WAS BAKED OUT 2 HOURS, PURGED WITH PURIFIED GAS FOR ONE HOUR AND BACKFILLED TO 18 PSIG PRIOR TO ZERO TIME

INSTRUMENT HOOK-UP

FIG 31

FIG 32

POTASSIUM ANALYSIS

	MSA Quoted Analysis (ppm)	Incoming Analysis (ppm)	*Post Purification Analysis (ppm)
Job No.		N-164	N-244
O_2	--	20-24	14-24
Na	Present	100	--
Ca	1	less than 50	less than 50
Mg	5	10 to 100	10
Fe	1	less than 100	8
Ni	2	less than 100	less than 1
Cr	3	less than 100	2

*Subsequent to this analysis, the potassium was purified, filtered, repurified and refiltered

At 3580 hours, an immersion heater in the preboiler gave an indication of being grounded. A hole had developed in the heater cladding exposing the heater element to liquid metal. The heater was isolated from the electrical system and the test continued, using the one remaining immersion heater in the preboiler.

After 3625 hours (980 boiling hours) a leak in the superheat-boiler drain line, similar to the test-boiler failure, caused a termination of the test program. Initial analyses indicate a stress-rupture type of failure due to weakening of the Haynes-25 material, at the drain-line junction.

Complete post-test evaluations, now in progress, of the failure regions and corrosion studies of the entire system will be presented in reports TIM-825 and CNLM-5660.

Fig. 33 is a post-test X-ray of the test boiler, which gives no indication of failure in the boiler tube or the heater.

TEST BOILER X-RAY, POST-TEST

TOP VIEW

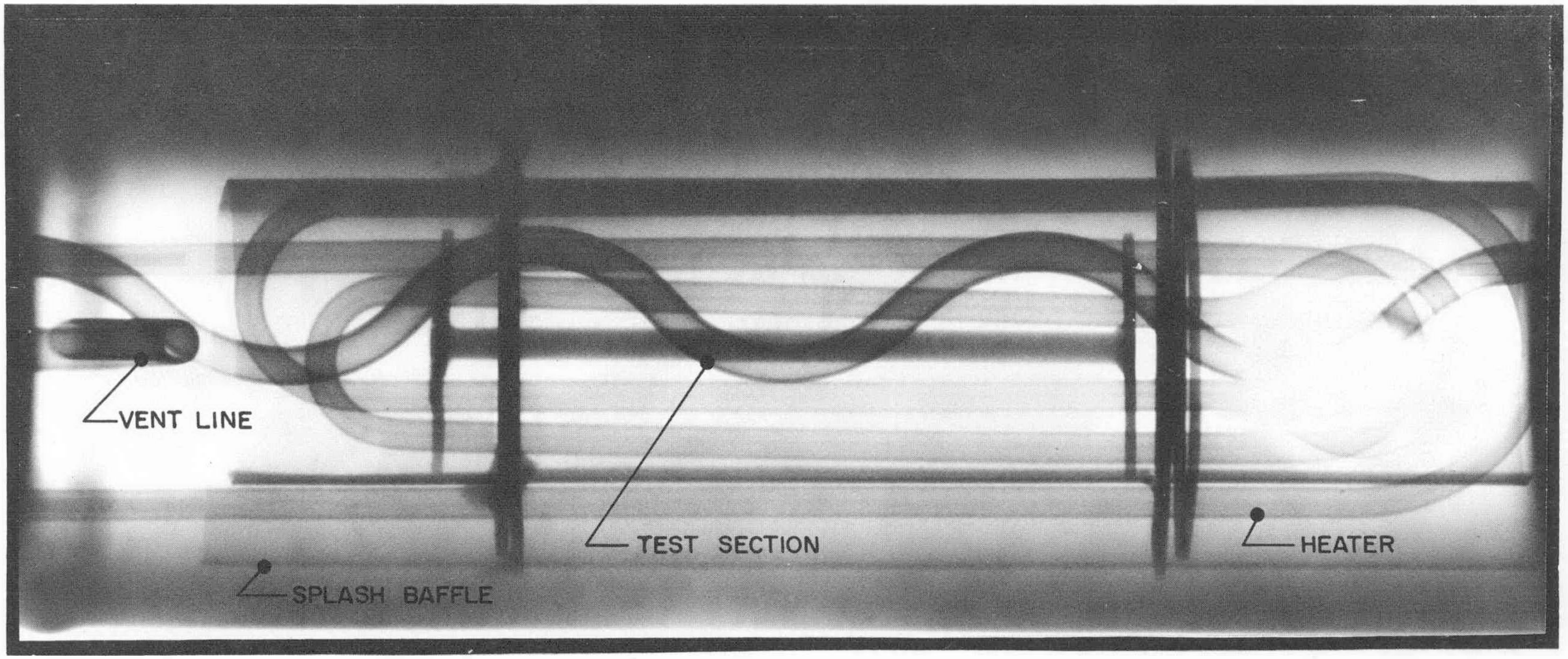

FIG 33

VIII. ANALOG STUDIES

(Reference 23)

A simplified electrical mock-up of the test loop was devised and constructed to establish the feasibility of using the analog computer as a tool in the design and operation of two-phase forced-convection systems. Actual performance of the test loop was compared with performance predicted by the analog. Areas of agreement between the experimental loop and the electrical analog were:

1. Subcooled nucleate boiling was simulated in the analog by superimposing a random noise (dirty diode) signal on the preheater inlet pressure. The noise signal caused pressure and flow perturbations. These perturbations were large at low qualities and small at high qualities. The positive slope of the heat transfer versus quality curve at low qualities caused a positive feedback loop, thus magnifying flow oscillations. The negative slope curve at high qualities caused a negative feedback system.

   Loop experience agreed with the analog as the magnitude of observed flow perturbations was less in the high quality regime than in the low quality regime.

2. Greater stability was predicted for high exit qualities. This agreed with the over-all operating experience.

3. It was predicted that throttling was needed at the preheater inlet to obtain stability. This was also confirmed in the experiment (Section VI-C-4).

4. The direction of pressure and flow changes as a result of a change in preheater power was predicted and demonstrated for both fixed-inventory and variable-inventory systems. This is shown below:

	Variable Inventory Soft System	Fixed Inventory Hard System
Power change	+	+
Boiler Exit Pressure	+	+
Condenser Exit Pressure	-	+
Condenser ΔP	+	+
Flow	-	-

In a hard system, a power change caused more significant changes in the system pressure level than in a soft system.

IX. CONCLUSIONS AND RECOMMENDATIONS

A. Heat Transfer

1. The performance of this tube did not start to deteriorate until about 85 percent vapor quality (Fig. 3). A straight tube indicates a performance drop at 60 percent quality (Ref. 22).
2. To properly size liquid metal boilers, it is necessary to obtain data using liquid metals. Water or other fluids can be used to indicate trends, (Fig. 22).
3. This experimental technique is excellent for obtaining local data, being versatile, reliable, and accurate.
4. The heat transfer data obtained in this experiment represents a significant start. Additional work is necessary and should be done at higher ΔT driving forces, and above average tube sizes and geometries.

B. Pressure Drop

1. The measured pressure drop bounds the calculated pressure drop (Martinelli-Lockhart correlation) by ± 20 percent (Fig. 4).
2. The pressure drop for the serpentine tube is 24 percent greater than for a straight round tube.
3. The pressure drop in a boiler significantly affects the size of a boiler since the integrated driving force (ΔT) is appreciably influenced by the reduction in saturated temperature.

C. Stability

1. Subcooled nucleate boiling appeared to create most of the instability experienced in this loop. Flashing orifices in the boiler are considered as the best method of solution. The choking effects expected in some types of orifices indicate potassium orifice tests are necessary.
2. Presence of noncondensible gas seemed to have an adverse effect on loop stability.
3. The condensing instabilities observed in the forced convection near horizontal (2 degrees upward) condenser indicates additional effort is needed to investigate the remedy for this problem.
4. The loop was most stable at high vapor qualities.
5. A fixed-inventory system was slightly more stable than a variable inventory system, but pressure control was more sensitive.
6. Stability of two-phase potassium systems cannot logically be studied with water or other common fluids because of liquid superheat requirements. These are functions of the amount of noncondensibles present, system purity, and the fluid properties of surface tension and thermal conductivity.

D. General

1. 50F to 70F of liquid superheat was necessary to initiate boiling.
2. Analog techniques promise to be a valuable tool in the understanding and operation of two-phase systems and in defining stable regimes. The operation of a Rankine Cycle in space by computer techniques requires that a conscientious effort be made to develop this valuable tool.

X. REFERENCES

1. Wright, Roger Maurice, "Downflow Forced-Convection Boiling of Water in Uniformly Heated Tubes", (Ph.D Thesis), UCRL 9744, August 21, 1961.
2. Polomik, E. E., Levy, S. and Sawochka, S. G., "Heat Transfer Coefficients with Annular Flow During 'Once-Through' Boiling of Water to 100% Quality at 800, 1100, and 1400 psi",GEAP 3703.
3. Kardys, C. F., "Boiling Inside Tubes to High Quality, " Pratt & Whitney Aircraft, (Preliminary Issue).
4. Liquid Metal Heat Transfer Programs, AiResearch Manufacturing Company. Presented by James J. Killackey at the Brookhaven Heat Transfer Conference in April 1962.
5. Noyes, R. C., "An Experimental Study of Sodium Pool Boiling Heat Transfer", NAA-SR-6769.
6. Sani, R. L., "Downflow Boiling and Nonboiling Heat Transfer in a Uniformly Heated Tube", UCRL 9023.
7. Nuclear Engineering, Edited by C. F. Bonilla, 1957, McGraw-Hill Book Co.
8. Heat Transmission, William H. McAdams, 1954, McGraw-Hill Book Co.
9. WADD Technical Report 61-96, Properties of Inorganic Energy Conversion and Heat Transfer Fluids for Space Applications.
10. Huber, D. A. and Hoehne, J. C., "Pool Boiling Investigation of Benzene, Diphenyl, and Benzene-Diphenal Mixtures under Pressure", NAA-SR-6681.
11. Griffith, P. and Wallis, J. D., "The Role of Surface Conditions in Nucleate Boiling", AICHE Preprint 106 presented at the Third National Heat Transfer Conference ASME-AICHE, Aug. 9 - 12, 1959.
12. Harrison, W. B. and Levine, Z., "Wetting Effects on Boiling Heat Transfer", AICHE Paper 57-HT-29.
13. Mumm, J., "Heat Transfer to Boiling Water Forced Through a Uniformly Heated Tube", ANL-5276.
14. Alman, M., Norris, R. H. and Staub, F. W., "Local and Average Heat Transfer and Pressure Drop for Refrigerants Evaporating in Horizontal Tubes", Trans. Am. Soc. Mech. Engrs. Ser. C, J. Heat Transfer 82, 189 (1960).
15. Hoffman, H. W. and Krakoviak, A. J., "Forced Convection Saturated Boiling of Potassium at Near Atmospheric Pressure", ORNL Report.
16. E. Bernstein, "Engineering Report on the Design of the Pratt & Whitney Aircraft Forced Convection Alkali Metal Vaporization-Condensation Heat Transfer Rig", CNLM-4358, January 18, 1963.
17. M. Jacobs and J. Hawkins, "Elements of Heat Transfer and Insulation, John Wiley & Sons, April, 1954.
18. J. Petrek, "Operating Instructions for the Forced Convection Alkali Metal Vaporization-Condensation Heat Transfer Rig", CNLM-5047, May 22, 1963.
19. Alkali Metals Boiling and Condensing Investigations, NASA Contract NAS-3-2528, NAS-5681, General Electric.
20. S. Fanciullo, "Thermocouple Development, Lithium Cooled Reactor Experiment", PWAC-422, March, 1964.

21. S. Fanciullo, "Development of Liquid Metal Level Probes", PWAC-423, April, 1964.

22. E. Bernstein, J. Petrek, J. Meregian, "Evaluation and Performance of Once-Through Zero Gravity Boiler Tubes with Two-Phase Water", PWAC-428, April, 1964.

23. Personal Communication with L. Beltracchi of P&WA.

24. Personal Communication R. Fritz, J. Horan, and D. Sadowsky of P&WA.

25. Correlation of Boiling Potassium Heat Transfer Data, TIM-832, Pratt & Whitney Aircraft, CANEL, June 16, 1964, D. Sadowsky.

APPENDIX A

EQUATION REPRESENTATION OF DATA

All the boiling heat transfer and pressure drop data obtained from the test boiler is best represented by the following equations:

Heat Transfer (x = fractional vapor quality, h_b = heat transfer coefficient, Btu/hr ft^2 F)

For $0 \leq x\ 0.2$

$h_b = 40,000\ x + 7000$

For $0.2 \leq x < 0.4$

$h_b = 10^4 \sqrt{\frac{x-0.055}{0.0645}}$

For $0.40 \leq x < 0.75$

$h_b = 25,420 - 1.187 \times 10^5 (x - 0.54)^2$

For $0.75 \leq x < 0.80$

$h_b = 75,700 - 74,000\ x_n$

For $0.80 \leq x < 0.85$

$h_b = 115,700 - 124,000\ x_n$

For $0.85 \leq x < 0.90$

$h_b = 125,900 - 136,000\ x_n$

For $0.90 \leq x < 0.92$

$h_b = 79,500 - 84,500\ x_n$

For $0.92 \leq x < 1.0$

$h_b = 275 \times 10^3 (1 - x_b)^2 + h_v$

Where h_v is calculated from Nusselt type forced convection equation using vapor properties.

Pressure Drop (ΔP in psi, flow = 17 lb/hr, ID = 0.186 inch, serpentine tube length = 14.98", equivalent straight length between pressure taps).

For $0.0 \leq x\ 0.50$

$\Delta P = 1.96\ x + 0.02$

For $0.50 \leq x \leq 1.0$

$\Delta P = 1.4\ x + 0.30$

APPENDIX B

NOMENCLATURE FOR BKHT-1 SAMPLE CALCULATIONS

A = Heat transfer area, ft^2
C_P = Specific heat, Btu/lb F
C = Nusselt equation constant, 0.725
D = Outer diameter of tube on which condensing occurs, ft.
g = Gravitational constant, $418 (10^6)$ ft/hr^2
h = Local boiling heat transfer coefficient, Btu/hr ft^2F
I = Immersion heater current, amps
K = Thermal conductivity, Btu-in/ft^2 hr F
L = Length, ft
P = Pressure, psia
ΔP = Pressure differential, psi
q = Heat flux, Btu/hr ft^2
Q = Heat flow, Btu/hr
U = Over-all boiling heat transfer coefficient, Btu/hr ft^2 F
r = Radius, ft.
t = Temperature, F
T = Temperature, F
ΔT = Temperature difference, F
V = Immersion heater voltage, volts
W_f = Mass flow, lb/hr
W = Immersion heater power, watts
X = Average vapor quality by weight
ΔX = Quality Change

Greek Symbols

λ = Latent heat of vaporization, Btu/lb
ρ = Density, lb/ft^3
μ = Viscosity, lb/ft hr

Subscripts

a = Atmospheric
B = Boiling
c = Condensing
h = Head effects
H = Haynes-25 alloy
i = Inside
o = Outside
L = Liquid metal
P = Preboiler
S = Superheat boiler
T = Test boiler
W = Wall

C/D = Condenser discharge
C/F = Condensing film
PI = Preboiler inlet
PS = Preboiler shell
PT = Preboiler tube
TS = Test boiler shell
TS = Tube to shell (when used with ΔP)
TT = Test boiler tube

Conversion Constants

a = 0.0903 psi/scale division (100% scale = 250" H_2O)
b = 0.1805 psi/scale division (100% scale = 500" H_2O)
c = 0.0361 psi/scale division (100% scale = 100" H_2O)
d = 3.413 Btu/hr watt
e = 0.23 psi/F (slope of "K" vapor pressure curve)

Pressure Locations

P3 - Condenser discharge pressure
P4 - Preboiler cavity shell pressure
P4K - Preboiler shell pressure converted to "K" Pressure
P5 - Test boiler cavity shell pressure
P7 - Preboiler tube side pressure drop
P8 - Test boiler tube side pressure drop
P9 - Superheat boiler tube side pressure drop
P10 - Condenser pressure drop
P21 - Test boiler shell to tube pressure differential

SAMPLE CALCULATIONS FOR BKHT-1

Sample Calculations for BKHT-1 using Run No. 19. Physical properties were obtained from Ref. 9.

I. "K" loop flow.

From flowmeter calibration curve (Fig. 14) at 0.1375 mv.

$$W_f = 17.32 \text{ lb/hr}$$

II. The system pressure distribution can be determined from gage readings corrected for atmospheric and head effects.

A. Condenser discharge pressure (psia)

$$P_C/D = P_3 + P_a + Ph_3$$

$$P_C/D = 48.84 \text{ psia}$$

B. Condenser pressure drop (psi)

$$\Delta P_c = (P10 - P_{h10})a$$

$$\Delta P_c = 2.94 \text{ psi}$$

C. Boiler tube-side pressure drop (psi)

1. Preboiler

$$\Delta P_p = (P_7 \text{ x b}) + P_{h7}$$

$$\Delta P_p = 4.11 \text{ psi}$$

2. Test Boiler

$$\Delta P_T = (P_8 \text{ x C})$$

$$\Delta P_T = 1.64 \text{ psi}$$

3. Superheat Boiler

$$\Delta P_S = (P_9 \text{ x b})$$

$$\Delta P_S = 5.31 \text{ psi}$$

D. Preboiler inlet pressure (psia)

$$P_{PI} = P_{C/D} + \Delta P_C + \Delta P_S + \Delta P_T + \Delta P_P$$

$$P_{PI} = 62.85 \text{ psia}$$

E. Boiler shell-side pressure (psia)

1. Preboiler

From the Experimental Relation of Potassium and Sodium Vapor Pressures (Fig. 25) and $(P_4)_{Na}$ = 15.4 psig

$$P_{4K} = 57.0 \text{ psig}$$

$$P_{PS} = P_{4K} + P_a + P_{h4}$$

$$P_{PS} = 71.72 \text{ psia}$$

2. Test Boiler

$$P_{TS} = P_5 + p_a + P_{h5}$$

$$P_{TS} = 73.12 \text{ psia}$$

F. Boiler average tube-side pressure(psia)

1. Test Boiler

$$P_{TT} = P_{C/D} + \Delta P_C + \Delta P_S + \frac{\Delta P_T}{2}$$

$$P_{TT} = 57.92 \text{ psia}$$

G. Test boiler, shell-to-tube pressure differential

$$\Delta P_{TS} = P_{TS} - P_{TT}$$

$$\Delta P_{TS} = 15.2 \text{ psi}$$

III. The boiler heat fluxes can be determined from power measurements on immersion heaters.

A. Preboiler

$$W_P = V_P I_P$$

$$W_P = 3940 \text{ watts}$$

$$q_P = \frac{W_P \times d}{A_P}$$

$$q_P = 50,200 \text{ Btu/hr ft}^2$$

B. Test Boiler

$$W_T = 205.7 \text{ watts}$$

$$q_T = \frac{W_T}{A_T} \times d$$

$$q_T = 16,570 \text{ Btu/hr ft}^2$$

IV. Preboiler Over-all Coefficient

A. Preboiler heat to preheat liquid to saturation temperature

$$Q_P = W_f C_P (T_b - T_1)$$

$$Q_P = 738 \text{ Btu/hr}$$

B. Preboiler heat to vaporizing liquid

$$Q_B = Q_T - Q_P$$

$$Q_B = 12,610 \text{ Btu/hr}$$

C. Preboiler exit quality

$$X_P = \frac{Q_B}{W_f \lambda}$$

$$X_P = 0.896$$

D. Preboiler over-all heat transfer coefficient

$$U_P = \frac{Q_P}{T_{PS} - T_{PT}}$$

$$U_P = 1041 \text{ Btu/hr ft}^2 \text{ F}$$

V. Test Boiler local heat transfer coefficient

A. Quality change in test boiler

$$\Delta X_T = \frac{Q_T}{W_f} \qquad X_T = X_{PT} \frac{\Delta X_T}{2}$$

$$\Delta X_T = 0.0496 \qquad X_T = 0.921$$

B. Local heat transfer coefficient

1. Temperature difference from shell to tube can be corrected for wall temperature drop (ΔT_W) and condensing film temperature drop ($\Delta T_{C/F}$).

   a. Wall Temperature Drop

   Equation for heat conduction through a homogeneous cylinder wall is

$$Q = \frac{2\pi L \; K_H (t_i - t_o)}{\ln r_o/r_i} = q_T \, A_T$$

$$\frac{2\pi L \; K_H \; \Delta T_W}{\ln r_o/r_i} = 2\,\pi L \; r_i \; q_T$$

$$\Delta T_W = \frac{r_i \ln r_o/r_i}{K} \; q_T$$

$$\Delta T_W = 1.45 \times 10^{-4} \, q_T$$

for $q_T = 16,570 \text{ Btu/hr ft}^2$

$$\Delta T_W = 2.4 \, ^\circ\text{F}$$

   b. Condensing Film Temperature Drop

   Nusselt's theory of film condensation on a horizontal tube (Ref. 17) and Newton's law of cooling ($Q = hA\Delta t$) can be applied to obtain an approximation.

$$\frac{hD}{K} = C \left(\frac{g\rho^2 \lambda D^3}{K_L M \Delta T_{C/F}} \right)^{1/4}$$

$$h = \frac{Q/A}{\Delta T_{C/F}}$$

   Using these equations, a condensing film temperature drop of 1.0F at a heat flux of 20,000 Btu/ft^2 hr was determined. This correlation is applicable to condensing metal vapors at 102 Reynolds Moduli which occur in this case.

2. For high tube-to-shell temperature differences, the shell cavity and average tube temperatures can be obtained from potassium vapor pressure at their recorded pressures.

$$T_{TS} = 1769 \text{ at } P_{TS} = 73.12 \text{ psia}$$

$$T_{TT} = 1704F \text{ at } P_{TT} = 57.92 \text{ psia}$$

$$\Delta T_B = T_{TS} - T_{TT} - \Delta T_W - \Delta T_{C/F}$$

$$\Delta T_B = 62.5F$$

$$h_T = \frac{q_T}{\Delta T_B}$$

$$h_T = 265 \text{ Btu/hr ft}^2\text{F}$$

3. For low tube-to-shell temperature differences, a shell-to-tube differential pressure measurement* can be used to determine this small differential. For Run No. 1-16,

$$\Delta T_B = \frac{(P21 \text{ x } a) + \Delta P_T/2}{e} - T_W - \Delta T_{C/F}$$

$$\Delta T_B = 32F$$

$$h_T = \frac{qT}{\Delta T_B}$$

$$h_T = 563 \text{ Btu/hr ft}^2\text{F}$$

*For greater accuracy, the differential pressure scale was set at 0 - 250" H_2O. Therefore, this calculation can be made for temperature differences less than 40F.

APPENDIX C
(Reference 24)

BOILING HEAT TRANSFER CORRELATION

In order to generalize the many types of data from many sources, a continuing attempt to correlate available information has produced some promising results.

Available data was plotted and cross plotted until a significant parameter was established. The results of this effort are shown in Fig. 34. This work was then extended to 100 percent vapor quality when all the data from this test was obtained. This empiricism is described in Fig. 35. A comparison with actual data is shown in Fig. 36.

If this work continues to look promising, a report will be circulated describing the correlation in more detail.

NUCLEATE BOILING CORRELATION

THIS CORRELATION IS FOR NUCLEATE BOILING ENTERING AT BOILING POINT AND "O" QUALITY, AND LEAVING AT "X" QUALITY

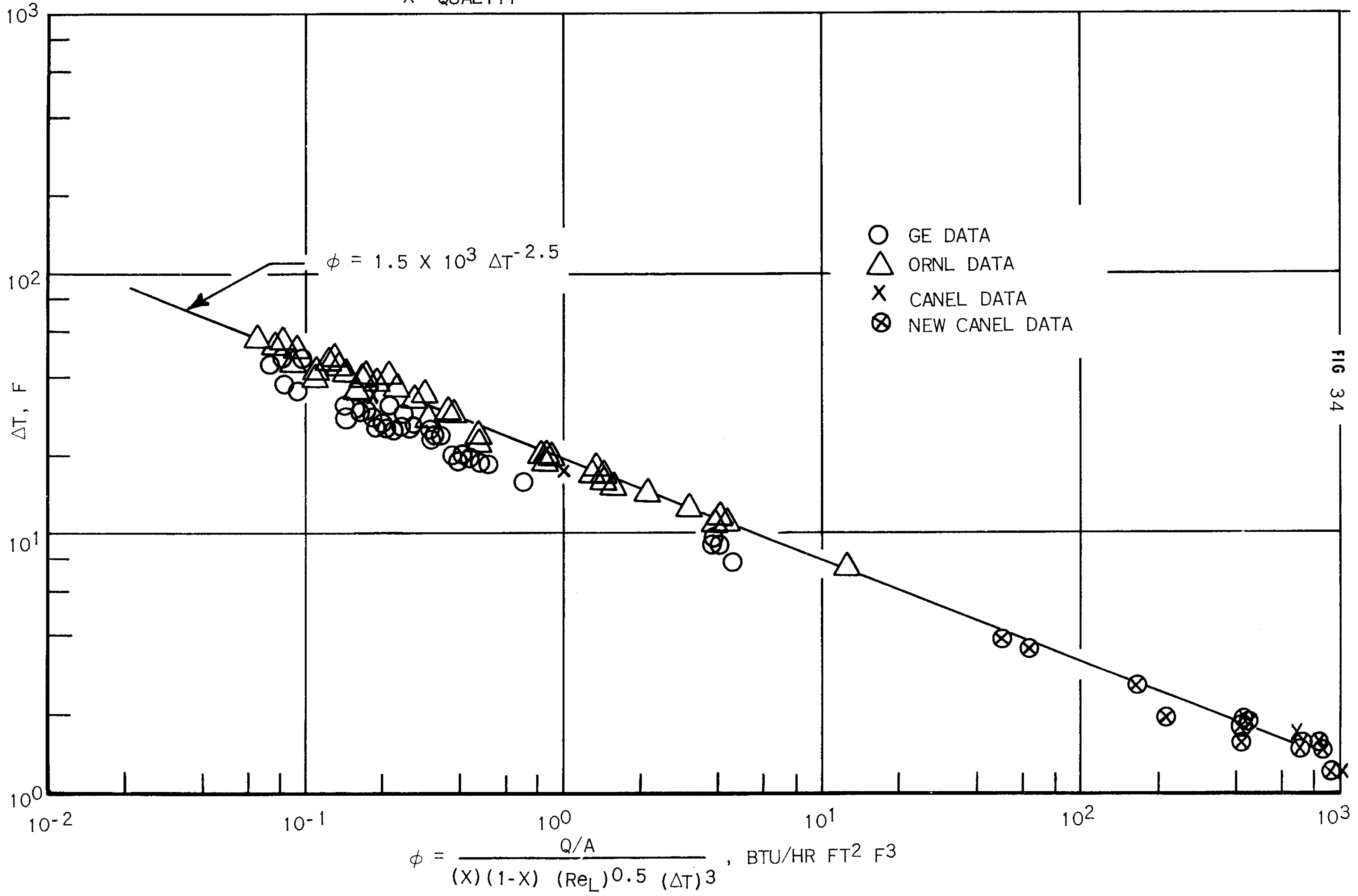

FIG 34

FIG 35

FULL RANGE BOILING CORRELATION

$$h_{local} = h_L(1-x) + h_g x + h_{TPF}(x)\,(1-x)^{(1)}$$

where:

$$h_L = h_1 + (\text{Chen})\,\Delta T_{film}, \quad \frac{h_1 D}{K_1} = 5.0$$

(Chen)$^{(2)}$ is a coefficient of bubble contribution dependent on physical properties for potassium

T °R	(Chen)
1660	270
1860	450
2060	690
2260	980

$$h_g = c_1 c_2 h_2, \quad \frac{h_2 D}{K_g} = 0.023\, N_{Reg}^{\,0.8}\, N_{Prg}^{\,0.4}$$

$c_1 \doteq 1$, roughness and/or curvature contribution

$c_2 \doteq 3$, upstream condition contribution$^{(3)}$

$$h_{TPF} = c_3\, N_{Re_{TPF}}^{\frac{1}{2}} \left(\frac{T}{\Delta T_{film}}\right)^{1/2}$$

c_3 = dimensional constant 14.0 Btu/hr-ft^2-F

$$N_{Re_{TPF}} = \frac{\text{inertia forces}}{\text{viscous forces}} = \frac{\left[\frac{G}{\rho_L}\left\{1 + x\left[\left(\frac{\rho_L}{\rho_g}\right)^{2/3} - 1\right]\right\}\right]^2 \frac{1}{R_o} + g}{\frac{\mu_L G}{D^2 \rho_L^{\,2}}\left\{1 + x\left[\left(\frac{\rho_L}{\rho_g}\right)^{2/3} - 1\right]\right\}} \quad \text{from}$$

$$\frac{V_g}{V_L} \doteq \left(\frac{\rho_L}{\rho_g}\right)^{1/3}$$

(1)Major groupings shown in Fig. 34.

(2)Chen, J. C. ASME Preprint 63-HT-34. Also Brookhaven National Lab Report BNL 7319.

(3)This increase in gas coefficient is believed to be caused by shear between liquid droplets and vapor. No correlating description of this surviving turbulence contribution is available.

FIG 36

COMPARISON OF EXPERIMENTAL DATA WITH FULL RANGE BOILING CORRELATION